

MarScC
GC856
0735
no. 75-18
cop. 2

School of
OCEANOGRAPHY



**Time Series of Temperature
Microstructure in the Arctic Ocean**

by

D. E. Amstutz
V. T. Neal

Reference 75-18
October 1975

OREGON STATE UNIVERSITY

Final Technical Report
Arctic Institute of North America

GC 856
0735
no. 75-18
cop. 2
man sc C

TIME SERIES OF TEMPERATURE MICROSTRUCTURE
IN THE ARCTIC OCEAN
March - April 1970

D.E. Amstutz* and V.T. Neal
School of Oceanography
Oregon State University
Corvallis, Oregon 97331

* now with
Polar Oceanography Division
Naval Oceanographic Office
Suitland, Maryland 20023

Final Technical Report
Arctic Institute of North America
Project Number ONR 432
October 1975

School of Oceanography
Oregon State University

John V. Byrne
Dean

TABLE OF CONTENTS

INTRODUCTION	1
EXPERIMENTAL DESIGN	2
TEMPERATURE OBSERVATIONS AND THERMISTOR CALIBRATION	8
STATISTICAL ANALYSIS	18
RECOMMENDATIONS	51
<i>ACKNOWLEDGMENTS</i>	53
<i>REFERENCES</i>	54

LIST OF FIGURES

1	Sensor Array	4
2	Configuration of the Array While Launching Through the Sea Ice	5
3	Experiment Time Schedule	10
4	Positions of T-3 During the Measurement Period	11
5	Linearized Profiles of Temperature and Salinity	13
6	Phase I Basic Temperature Statistics	21
7	Phase I (Temperature $-\bar{T}$) 10^4 °C For Every 10th Sample Value ...	22
8	Phase I Probability Density Functions For Channels 1,3,4, and 6	25
9	Phase I Probability Density Functions For Channels 7,8,9 and 10	26
10	Phase III(b) File 3 Probability Density Function For Channel 10	27
11	Phase I Average Normalized Spectrum For Channels 1,6,7,8,9 and 10	31
12	Phase II Temperature Statistics	33
13	Phase II (Temperature $-\bar{T}$) 10^4 °C For Every 10th Sample Value ..	34
14	Phase II Average Spectrum for Channels 3,4,6,7,8 and 9	36
15	Phase II Temperature Series (Temperature Values not Converted)	40
16	Phase III(a) Temperature Statistics	47
17	Average Normalized Spectrum for Phase III(a)	49

LIST OF TABLES

I	Phases of Temperature Measurement Program	12
II	Computation of Field Calibration Constants (°C)	16
III	Accepted Mean <u>in situ</u> Temperatures for all Phases	17
IV	Standard Deviations of Recorded Temperatures, Phase III(b). Files 1 through 3, All Channels (10^{-4} °C)	19
V	Summary of Temperature Statistics (°C)-Phase I	23
VI	Summary of Temperature Statistics (°C)-Phase II	32
VII	Phase III(a)-Plateau Removal (°C)	43
VIII	Magnitude of Temperature Plateau (°C)	44
IX	Summary of Temperature Statistics (°C) Phase III(a)	45

I. INTRODUCTION

The microstratification found at many places in the oceans has been well documented in recent years (Stommel and Fedorov, 1967; Cooper, 1967; Woods, 1968; Lovett, 1968; Tait and Howe, 1968). Our Arctic studies have revealed that microstructure is common there. We have observed in deep water (at least in the Canadian Basin) several interesting aspects of it (Neal, Neshyba and Denner, 1969; Neshyba, Neal and Denner, 1971 and 1971a, 1972; and Neal and Neshyba, 1972). The same phenomenon of stratification has been produced in the laboratory by several workers (Turner and Stommel, 1964; Turner, 1965, 1967, 1968). In general the differing diffusivities of heat and salt are called upon to explain the formation of microstructure. However, since layering also appears in freshwater lakes (Neal, Neshyba and Denner, 1971) some other mechanism must be capable of producing it.

We designed an experiment to see if turbulence induced by shear instability could be a mechanism. Using equipment readily available we completed an experiment from the Ice Island T-3. A sensor array of current meters and thermistors (described later on) was suspended beneath the sea ice of Colby Bay, T-3, and data were recorded for 37 days during March and April, 1970. Our goals were: 1) to compute vector differences among current meter records and correlate them with temperature differences among the thermistors; 2) to run a spectral analysis of current meter and temperature records for determination of the partitioning of energy between long and short periods; 3) determination of statistical coherence among the current meter records; and 4) determination of temporal and spatial (vertical) sampling necessary for studies of turbulent processes which may act within layers whether induced by shear instability or by breaking of internal waves.

The current meters did not function properly therefore no water velocity data were available. The thermistors and associated monitoring, digitizing and recording electronics did function however. So, we revised our objectives and concentrated on a descriptive examination of the temperature time series.

II. EXPERIMENTAL DESIGN

The original experiment called for use of both current meters and thermistors. This section describes the complete experiment, including the current meter array. The design, configuration and equipment deployment/recovery techniques are considered to be of value to future experimenters and therefore are described in some detail.

The experiment was planned to obtain simultaneous measurements of temperature and water velocity along a limited vertical profile centered at specific depths which were selected on the basis of the observed vertical temperature and salinity gradients. Specifically, we desired to install the array at the boundary between Arctic surface water and Atlantic water where the vertical gradients of both temperature and salinity are relatively large and positive (increasing concentrations of heat and salt with increasing depth). Additional measurements were also made at the lower boundary of the Atlantic water where the vertical salinity gradient is nearly zero and the vertical temperature gradient is negative.

The sensor array included both current meters and thermistors. They were spaced to adequately sample the microstructure in the Arctic Ocean. A vertical scale of about one meter was believed adequate. It was essential that each thermistor be at the same depth as its corresponding current meter. We were to utilize available equipment. It was necessary to deploy and retrieve this equipment through a hole in the sea ice of Colby Bay (T-3).

The configuration of the complete array is shown in Figure 1. Configuration of the array during launch is shown in Figure 2. The original current direction vanes of the Braincon Type 381 histogram current meters were modified to accommodate launch and recovery through the sea ice and to restrict their vertical dimension. The vanes were modified to provide the same dynamic characteristics as the originals. During launch the vanes were held in the upward position with a small string and a candy "Lifesaver". The time required for the candy to dissolve after being submerged was sufficient to deploy each current meter to a depth below the ice yet brief enough to allow visual confirmation that the vanes dropped into the horizontal position.

The current meters, manufactured by Braincon Corporation, Marion, Mass, are graphic photorecording instruments. Luminous sensor indicators of current speed and direction, tilt direction and amplitude are used to expose Kodak tri-X film. The Braincon type 381 unit employs a Savonius rotor magnetically coupled to a gear train which turns the speed indicator. The direction vane orients the pressure case and current directions are established with respect to local magnetic north. Timing of data acquisition is established with a Bulova Acutron clock. Mechanical contacts on these clocks activate the film advance motor. The film is exposed and advanced at 10 minute intervals.

As the primary experiment was designed for a duration of some 30 days, the Acutron clocks were operated for an equivalent time within a cold chamber prior to shipment north. These clocks were maintained at the anticipated Arctic Ocean water temperature and were situated within the cold chamber with the same orientation to be experienced when suspended beneath the sea ice of Colby Bay (T-3). The rate of advance or delay for each clock was thus established. These pre-deployment tests were conducted

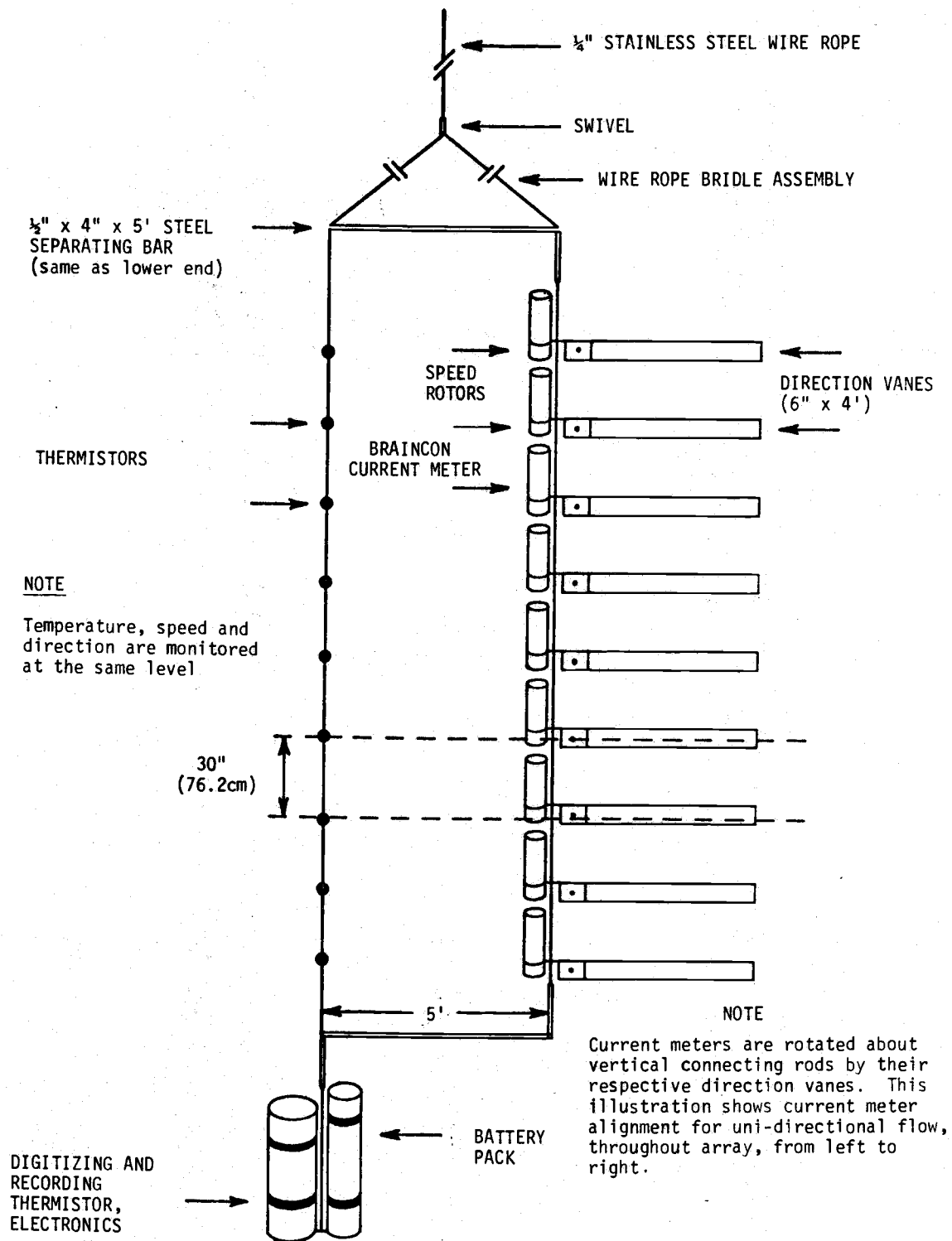


FIGURE 1
SENSOR ARRAY

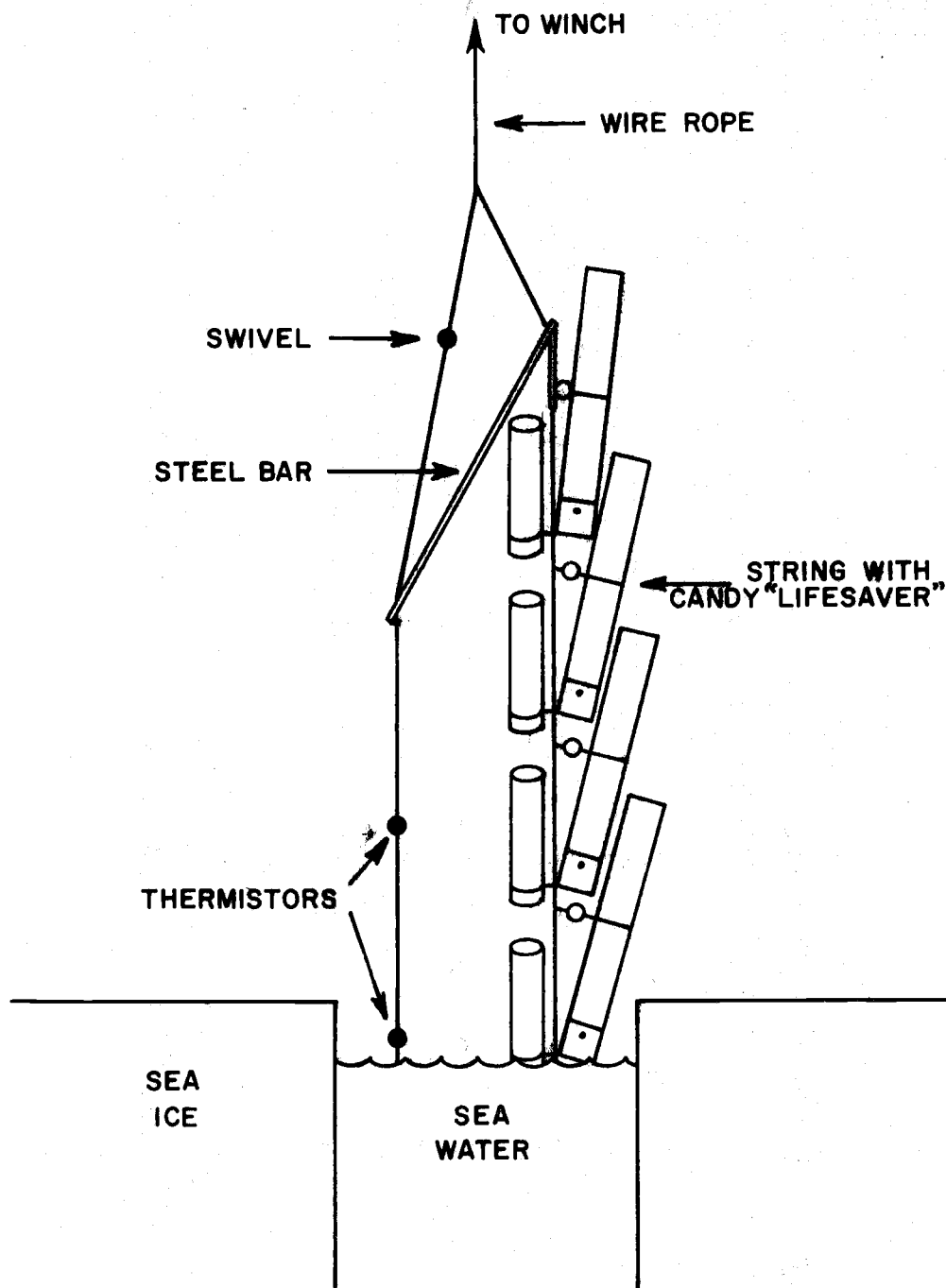


FIGURE 2
 CONFIGURATION OF THE ARRAY WHILE LAUNCHING THROUGH THE SEA ICE

to assure that data collected from each of the various sensors would lend itself to individual analysis as well as to group analysis with the data from the other sensors. This temporal compatibility among data records extends to the thermistors also.

The second portion of our sensor array consisted of thermistors, manufactured by Yellow Springs Corporation, and a digital automatic recording device constructed at Oregon State University. The thermistors, Yellow Springs type 44031, were connected to the digital recorder with waterproof connectors and cables. The cables were fabricated to the array dimensions at OSU. The digitizing and recording unit, identified by the acronym DART (Digital Automatic Recording Thermistor) consists of a Wheatstone bridge circuit, a sequencing selector which scans the thermistors making up the vertical array, a digitizer and a magnetic tape recorder. Power for the DART is supplied from batteries contained within a pressure case bolted to the DART. The sampling rate of 10 minutes was controlled by a Bulova Acutron clock, identical with those which controlled the sampling rate of the current meters. An optional sampling rate of 2.5 seconds is available with the DART. This circuit, which by-passes the clock, was the most rapid sampling rate available to us. Some data were taken at this rate to extend our analysis to higher frequencies. Through control of the duration of each portion of the experiment we were able to analyze temperature fluctuations with periods from a few seconds to several days.

The thermistors were calibrated at OSU prior to deployment. A field calibration, performed during the last stages of the experiment, is at variance with the resistance versus temperature data acquired during laboratory calibration. This variance is believed to have resulted from

exposure of the thermistors to extreme cold even though the thermistors were hand carried to T-3 to help avoid such a problem. Temperatures within the trailers (living quarters aboard T-3) reached extreme lows prior to the experiment when the moisture in heating oil lines froze. The low temperatures were reached before repairs to the fuel lines could be made. The field calibrations are believed to be accurate to $\pm 0.02\text{C}^\circ$, based on the accuracy of the reversing thermometers used for this portion of the work.

The complete array (Figure 1) consisted of a string of current meters suspended parallel to the string of thermistors. These units were spaced in the vertical so that for each depth increment (76 cm) a speed rotor, direction vane and thermistor were located at precisely the same depth. Stability of the configuration or geometry of the array was assured through equipment design. The suspension line and bridle assembly was of quarter inch stainless steel wire rope. Swivels were placed at both ends of the suspension line. For launch and recovery the array was canted while it passed through the hole in the ice. The sensors were attached or removed at the upper surface of the ice due to the low ceiling height of the work hut. Recorder time was referenced to absolute time, in the case of the current meters, by inducing 90° tilts to the pressure cases; and in the case of the thermistors, by the extreme change in temperature between the atmosphere of the work hut and that of the sea water.

It was felt that with the sensor array, configured as described above, we would be able to acquire not only time histories of temperature and water velocity at several closely spaced depths but also invaluable observations of vertical shear and a concomitant measure of the vertical density structure. Obviously, measurement of the vertical temperature structure alone would not reflect the important contribution to density of changes in salinity; but,

the estimates of density, based on temperature and pressure, would serve to establish the potential significance of Kelvin-Helmholtz instabilities in development and maintenance of the Arctic Ocean microstructure. In addition, we felt that the data acquired from the sensor array would lend themselves to analysis for vertical coherency and thus some reliable estimates of the vertical scales of the processes involved in development and maintenance of the microstructure.

III. TEMPERATURE OBSERVATIONS AND THERMISTOR CALIBRATION

As pointed out in the introduction, the current meters failed to function properly. The nine instruments failed for one or more of the following reasons: current speed rotors stuck shortly after the experiment began; film did not advance properly (if this occurs more than once on a single magazine of film one cannot establish a reference to real time except for those portions between the beginning and the first malfunction and between the last malfunction and the end); and the Acutron clock stopped. Some brief portions of the current meter data might lend themselves to analysis though the time required would be extensive and one would not be able to reference the observations to real time.

The need for referencing the current meter and temperature records to a common, in this case real, time is apparent. In order to assure this we arranged for the array to be raised for 10-20 minutes every five days during the 37-day experiment. The array was brought slowly upward and allowed to remain at a shallower depth for sufficient time so that all sensors were sampled. The array was then slowly returned to its initial position. This procedure induced changes in temperature sensed because of

the vertical temperature gradient. Rotation of the current meter direction vanes provided an event mark on the current direction portion of the photographic data frame.

The temperature data acquired from the array were suitable for detailed analysis. Temperature data were acquired on four occasions while the equipment was aboard T-3. For discussion purposes these occasions are referred to as Phases I through IV. During Phases I and II the thermistors and DART were lowered and operated without the current meter array. These data were acquired to examine relatively high frequency (1 to 10^2 cph) temperature fluctuations. Phase III(a) constitutes the primary experiment during which both thermistors and current meters were deployed on the array. The field calibration of the thermistors was performed during Phase III(b). For this work the thermistors were bundled into a cluster and data recorded at each of the three depths: 270m; 280m; and, 290m. During Phase IV the thermistors and DART were lowered to 600m. As mentioned above, this deeper region of the Arctic Ocean is characterized by a negative vertical temperature gradient and nearly zero vertical salinity gradient. A summary of the dates and times during which temperature data were acquired is presented in Table I and Figure 3. The locations of ice island T-3 during the measurement periods are shown in Figure 4.

At various times throughout the period of experimentation from T-3, oceanographic observations were obtained. These observations consist of temperature, salinity and depth (with Nansen bottles and reversing thermometers). Ocean station observations were acquired on a weekly basis during this period with sampling depths extending to approximately 250m. One

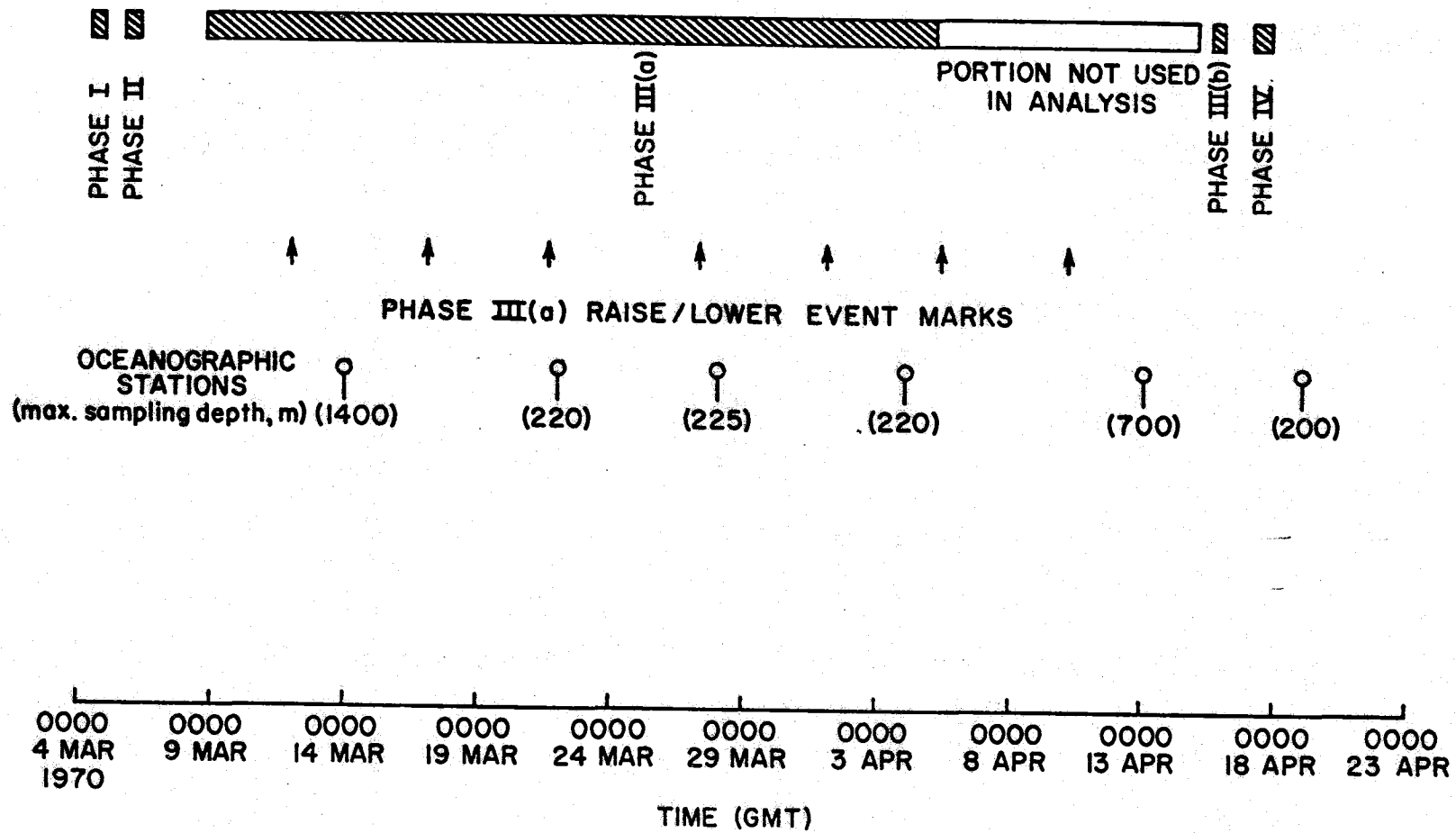


FIGURE 3
EXPERIMENT TIME SCHEDULE

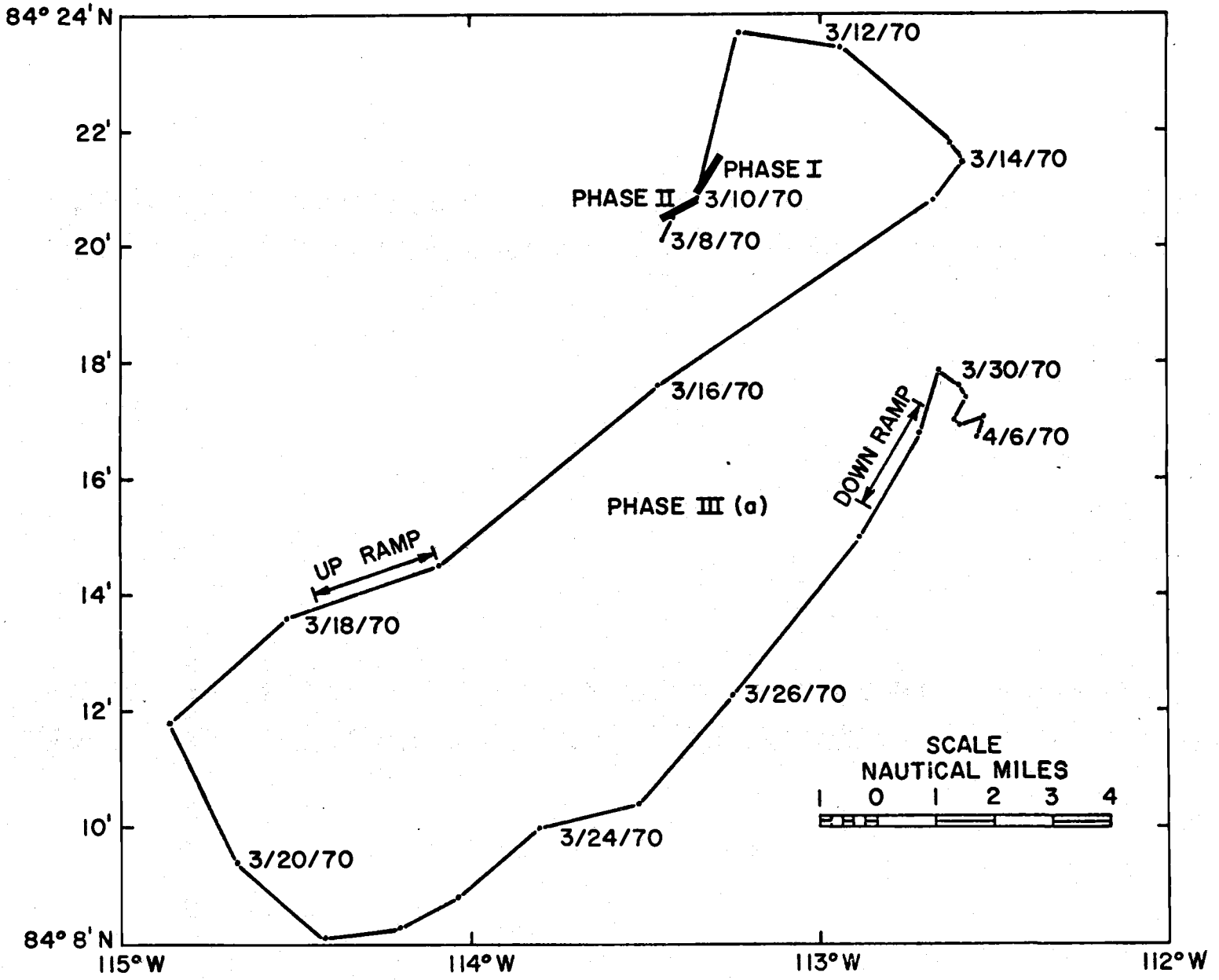


FIGURE 4
POSITIONS OF T-3 DURING THE MEASUREMENT PERIOD

ocean station per month was to acquire data to depths of approximately 1500m. The two deep stations for the months of March and April were considered in detail for determination of field calibration constants. After analysis, the best fit linear distributions of temperature and salinity versus depth (Figure 5) obtained on 13 April were chosen for use with the Phase III (b) clustered thermistor values, obtained on 15 April, to determine field calibrations constants for each thermistor. The positions of data acquisition may be determined from Figure 4 (14 March and 13 April, 1970).

TABLE I
PHASES OF TEMPERATURE MEASUREMENT PROGRAM

<u>Phase</u>	<u>Dates (GMT)</u>	<u>Approximate Duration</u>	<u>Nominal Sampling Interval</u>	<u>Configuration of Thermistor array</u>
I	4 Mar '70	10.5 hrs.	2.5 sec	Vertical; thermistors spaced 76.2 cm apart between depths of 276m and 282m
II	5 Mar '70	13.0 hrs.	2.5 sec	Vertical; thermistors spaced 76.2 cm apart between depths of 278 and 284m.
III(a)	8 Mar - 5 Apr '70	28 days	19.7 min	Vertical; thermistors spaced 76.2 cm apart between depths of 278m and 284m.
III(b)	15-16 Apr '70	8.5 hrs.	2.5 sec	Cluster; thermistors connected in a bundle and operated at depths of 270m, 280m and 290m.
IV	17 Apr '70	10.4 hrs.	2.5 sec	Vertical; thermistors spaced 76.2 cm apart between depths of 600m and 606m.

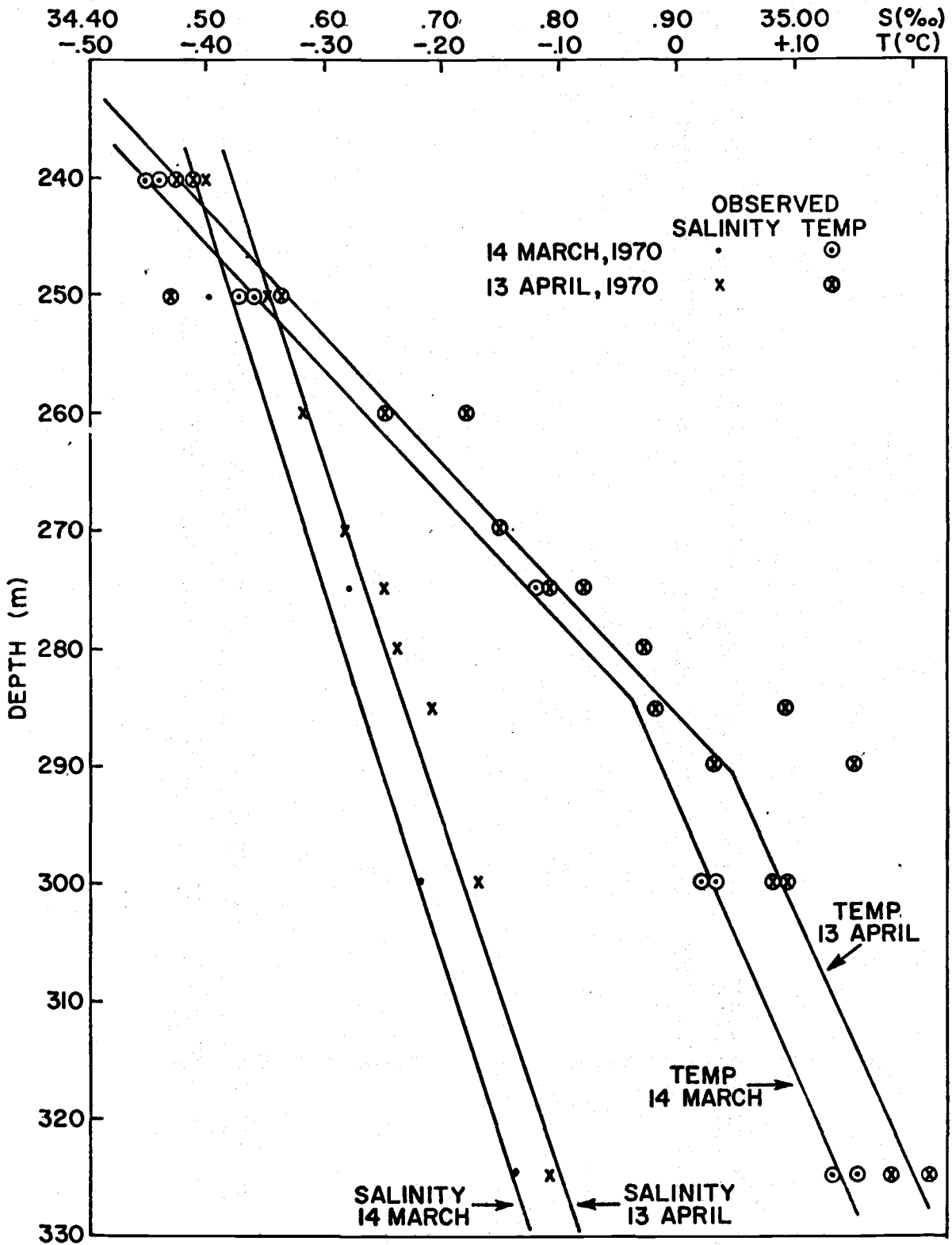


FIGURE 5
 LINEARIZED PROFILES OF
 TEMPERATURE AND SALINITY

The Phase III(b) thermistor values were categorized into three files, one for each of the depths of 267.5m, 277.5m and 287.5m. Each of these files contains 1000 consecutive observations. These observations were taken within the well-mixed layers and not within the regions of large vertical temperature gradient (sheets). Thus the thermistors were not influenced by rapidly changing temperatures during acquisition of the 1000 consecutive samples.

The temperature data are reported in terms of channel numbers. This naming procedure is chosen with the hope of being least confusing. Within the DART, resistance values are digitally recorded on magnetic tape on each of 10 channels. The thermistors were connected in such a way that their sampling depths (except Phase III[b]) increase with increasing channel numbers. Channel number 2 malfunctioned during the experiment and therefore, is not reported. Channel number 5 contains resistance values of an internal reference and thus is not reported.

To determine satisfactory field calibration constants, the temperature at 277.5m was read from Figure 5 (-0.080°C). The mean values obtained from each of the 8 channels of file 2 (277.5m depth) were set equal to an in situ temperature of -0.080°C . The necessary field calibration constants were computed and recorded in Table II. These constants, established for a depth of 277.5m, were then applied to each mean channel value of file 1 (267.5m) and file 2 (287.5m). The temperatures resulting for each channel were averaged for file 1 yielding an in situ temperature at 267.5m of -0.155°C . By the same process the in situ temperature at 287.5m was deduced to be $+0.002^{\circ}\text{C}$. Accepting the temperatures arrived at in this manner, individual channel calibration constants were computed for files

1 and 2 and recorded in Table II. These values for each channel do not vary among files by more than 0.001°C. The three calibration constants for each channel were then averaged and these average values accepted as the field calibration constant for the channel (Table II).

The accepted field calibration constants were utilized with the mean channel values for each of the other Phases to establish accepted in situ temperatures. The results are presented in Table III and may be used for determination of absolute (versus relative) temperature values.

It is acknowledged that the number of digits presented in Tables II and III are excessive. No claim is made that correct values of in situ temperatures are provided beyond the accuracy of the reversing thermometers ($\pm 0.02^\circ\text{C}$) used in obtaining the 13 April, 1970 vertical temperature profile. It is to be emphasized, however, that changes and differences in temperatures are more correct, certainly by one digit than the reversing thermometer values. The procedure of retaining digits until after completion of numerical operations is justified.

TABLE II

Computation of Field Calibration Constants (°C)

Channel Number	Mean Temp(°C) File 1 (267.5m)	Implied Field Cal. Const.	Mean Temp(°C) File 2 (277.5m)	Implied Field Cal. Const.	Mean Temp(°C) File 3 (287.5m)	Implied Field Cal. Const.	Accepted Field Cal. Const.
1	-.8065	.6515	-.7305	.6505	-.6481	.6501	.6507
3	-.8902	.7352	-.8151	.7351	-.7322	.7342	.7348
4	-1.0276	.8726	-.9514	.8714	-.8685	.8705	.8715
6	-1.0048	.8498	-.9290	.8490	-.8463	.8483	.8490
7	-.6744	.5194	-.6004	.5204	-.5195	.5215	.5204
8	-.7537	.5987	-.6787	.5987	-.5979	.5999	.5991
9	-.7009	.5459	-.6266	.5466	-.5452	.5472	.5466
10	-.6807	.5257	-.6056	.5256	-.5253	.5273	.5262

TABLE III

Accepted Mean in situ Temperatures for All Phases

Channel Number	Accepted Field Cal. Const.	Phase I (°C)	Phase II (°C)	Phase III (a) (°C)
1	.6507	-.1123	-.1004	-.1144
3	.7348	-.1077	-.0977	-.0896
4	.8715	-.0981	-.0876	-.0810
6	.8490	-.0936	-.0739	-.0724
7	.5204	-.0839	-.0675	-.0609
8	.5991	-.0730	-.0584	-.0555
9	.5466	-.0636	-.0452	-.0475
10	.5262	-.0522	-.0436	-.0426

The three files of 1000 values each, used for determination of the field calibration constants, were also analyzed for determination of the overall noise level of the DART. As mentioned above, these files were selected from the Phase III(b) records to represent a span of time during which the clustered thermistors were located within a well-mixed layer. Through examination of these 1000 values from each file it was apparent that the in situ temperatures were steady with respect to time.

The temperature values for each of the channels were analyzed using the following procedure: (1) select file; (2) select channel; (3) compute channel mean temperature; (4) subtract channel mean temperature from each observation; and, (5) compute variance and standard deviation. The resulting standard deviations are presented in Table IV.

Examination of Table IV reveals a maximum noise level of approximately $\pm .001^{\circ}\text{C}$. This value is the approximate level obtained from File 3. We feel that the smallest value, obtained from a single file, may be selected as the maximum noise level because the fluctuations in temperature reflect environmental changes as well as noise within the electronics. The latter term incorporates the inherent digitizing limits of the system.

IV STATISTICAL ANALYSIS

A. Phase I (4 March, 1970)

During this portion of the work the thermistor array was suspended between the depths of 276m and 282m. The nine thermistors were spaced vertically at intervals of 76.2m. (The second thermistor from the top, channel 2, provided no analyzable data.) The thermistors were sampled by the DART at a nominal rate of once each 2.5 seconds. There were 19,008

TABLE IV

Standard Deviations of Recorded Temperatures,
Phase III(b) Files 1 through 3, All Channels (10^{-4} °C)

Channel Number	File 1 (267.5m)	File 2 (277.5m)	File 3 (287.5m)
1	18.7	14.3	12.8
3	20.0	13.2	9.5
4	21.5	12.6	10.9
6	16.8	15.7	11.8
7	16.3	14.3	9.4
8	17.6	13.5	12.0
9	16.0	13.2	11.1
10	16.2	13.0	9.8

samples acquired from each of the 8 functioning thermistors. Data collection was initiated when battery power was connected to the DART and terminated when the magnetic tape was fully recorded or when battery power was disconnected. Since recording began before the array was placed in the water the maximum storage capacity of the magnetic tape could not be utilized during an experiment. However, because of the relatively large capacity of the tape, this limitation presented no difficulties.

A summary of basic statistics describing these observations are contained in Table V. They are also shown in Figure 6. The field calibration constants from Table III have been included in the third column.

The increase of temperature with increasing depth, characteristic of this region and depth interval of the Arctic ocean, is revealed through examination of the accepted mean temperature values. The vertical temperature gradient, based upon the accepted mean temperatures of the shallowest and deepest thermistors, is $0.00986^{\circ}\text{C m}^{-1}$. This mean vertical gradient is in excellent agreement with the linear gradient between 240m and 285m shown in Figure 5.

To better visualize the passage of the stepped vertical thermal structure within the array, every tenth observation from each of the thermistors was plotted. These observations are presented in Figure 7. The entire recording (all observations) has of course been examined to assure the validity of resampling at a nominal rate of one sample per 25 seconds (every tenth value). Since there were no valid data from channel 2 there is a gap between the observations denoted as channel 1 and channel 3.

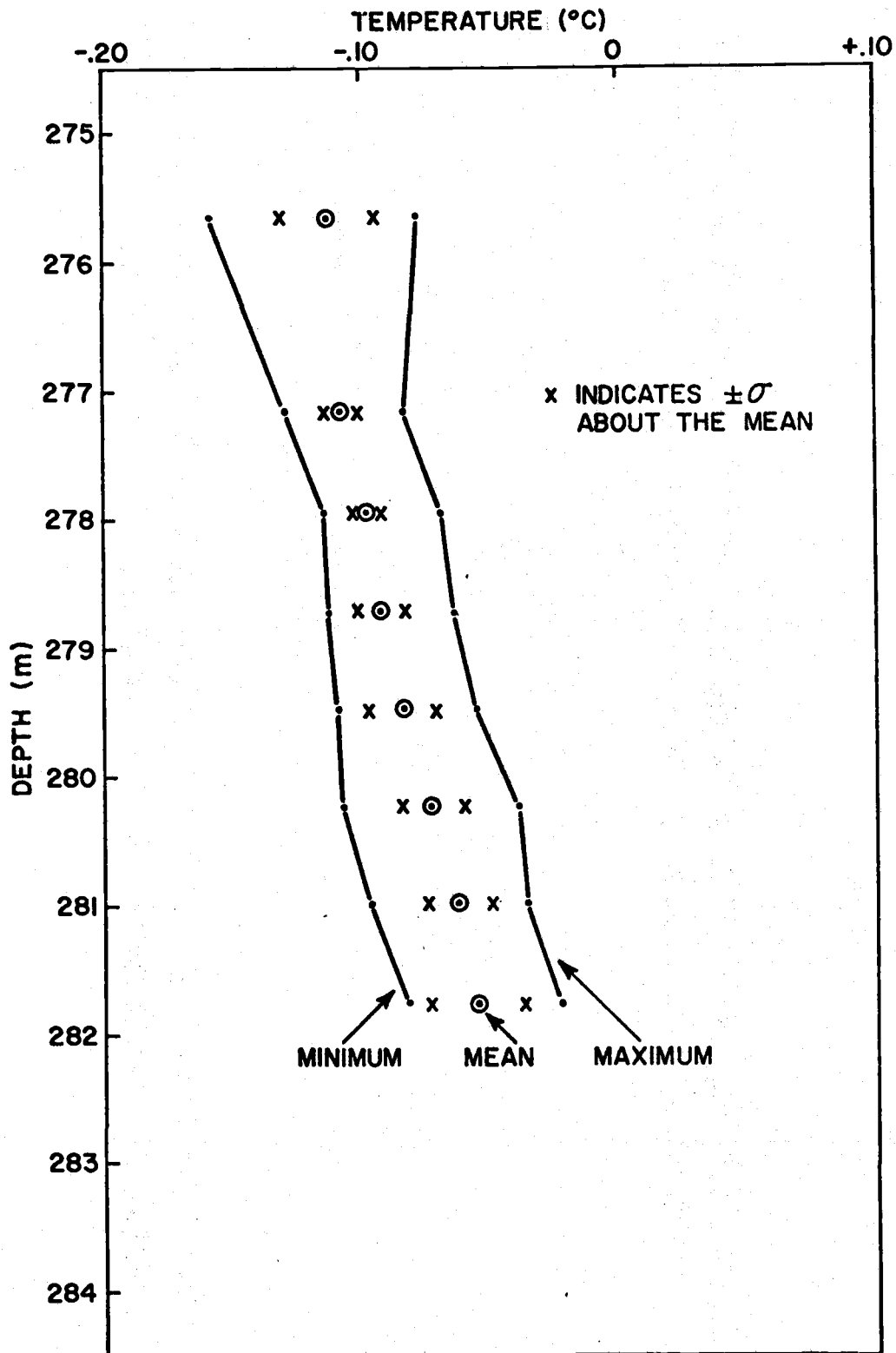


FIGURE 6
PHASE I BASIC TEMPERATURE STATISTICS

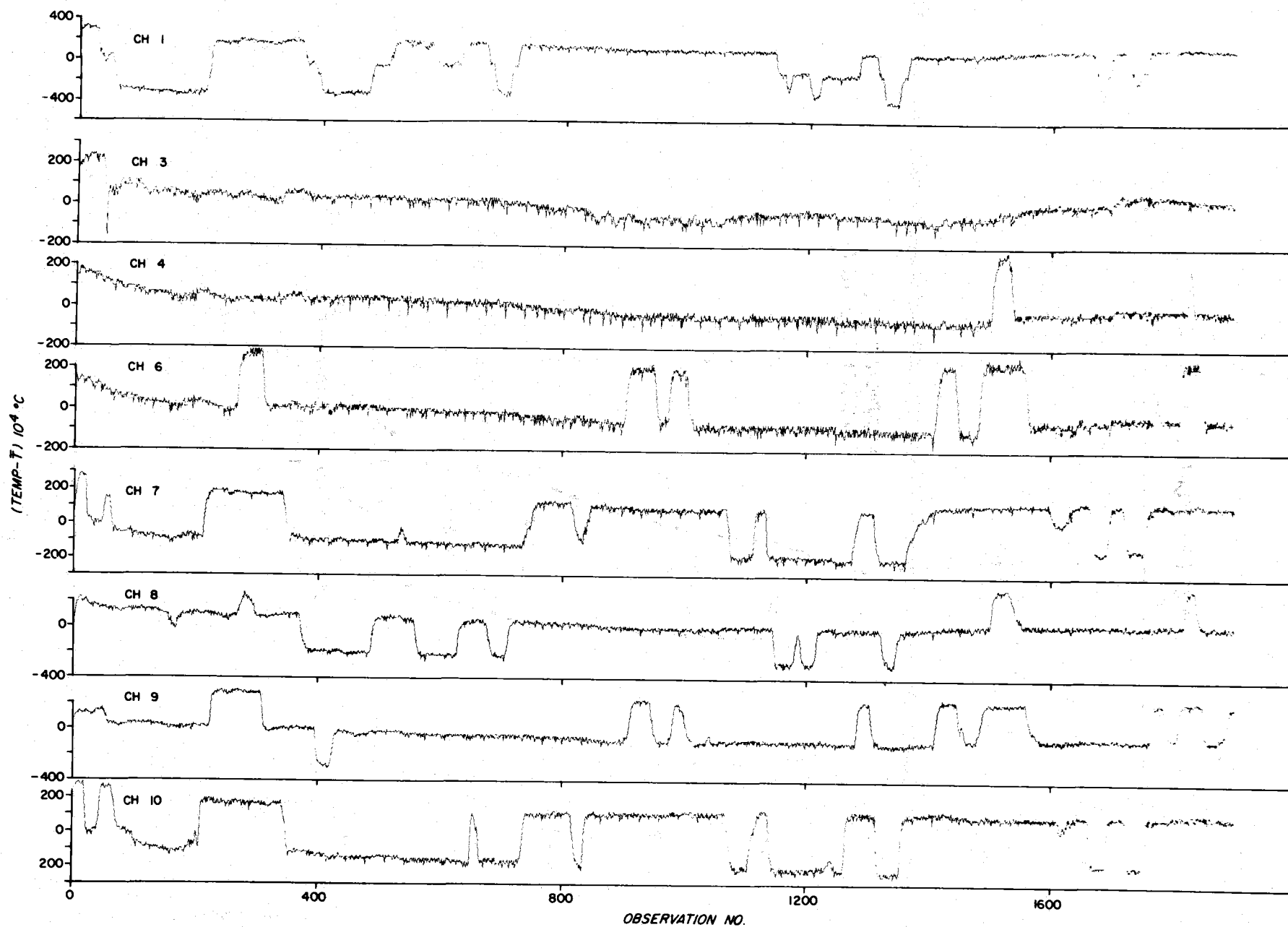


FIGURE 7

PHASE I (TEMPERATURE \bar{T}) 10^4 °C FOR EVERY 10th SAMPLE VALUE

Depth increases with increasing channel number. The ordinates of these plots vary with each channel. In keeping with our primary purpose of discussing relative changes in temperature we have, in many instances (as in Figure 7) removed the mean values. The ordinate values are, precisely, the observed temperatures minus the channel mean temperature value, multiplied by 10^4 .

TABLE V

Summary of Temperature Statistics ($^{\circ}\text{C}$) Phase I

Channel Number	Uncorrected Mean	Field Cal. Const.	Accepted Mean	Standard Deviation	Min. Temp.	Max. Temp.	Temp. Range
1	-.7630	.6507	-.1123	.0172	-.1582	-.0798	.0784
3	-.8425	.7348	-.1077	.0058	-.1288	-.0820	.0468
4	-.9696	.8715	-.0981	.0060	-.1132	-.0687	.0445
6	-.9426	.8490	-.0936	.0099	-.1121	-.0634	.0487
7	-.6043	.5204	-.0839	.0125	-.1091	-.0552	.0539
8	-.6721	.5991	-.0730	.0117	-.1070	-.0387	.0683
9	-.6102	.5466	-.0636	.0119	-.0965	-.0326	.0639
10	-.5784	.5262	-.0522	.0138	-.0808	-.0222	.0586
						average	.0579

The magnitudes of the steps in temperature, equivalent to the difference in temperature between vertically successive well-mixed layers, may be estimated from Figure 7 as follows: channel 1, 0.024°C; channel 3, no clearly defined steps; channel 4, 0.030°C; channel 6, 0.030°C; channel 7, 0.029°C; channel 8, 0.014°C; channel 9, 0.014°C; and, channel 10, 0.025 to 0.032°C. The approximate average value is 0.026°C. Using this average value, in conjunction with the temperature range resulting from the difference between the minimum temperature from channel 1 and the maximum temperature from channel 10, we concluded that there are approximately 5.3 vertical temperature steps within the depth interval sampled by the array. However, the temperature steps are not of equivalent values but encompass an approximate range of values between 0.014°C and 0.032°C. If there is a reasonably consistent value which might be assigned it may well be half of our average value, namely 0.013°C. Perhaps these initial steps merge in some fashion.

A third way of examining these data is by use of the probability density functions of each channel. These functions are shown in Figure 8 and 9. The values along the abscissae are observed values minus the mean, multiplied by 10^4 . From these figures one may estimate the relative amounts of time during which the thermistors were subjected to various in situ temperature domains. These density functions were computed using every tenth value from the original temperature records.

If an ideal thermistor were subjected to an absolutely uniform environmental temperature for the entire period of observation, most of the values, and hence probability, would be accumulated along a single line. A normal distribution, of relatively low mean value amplitude, would be superimposed

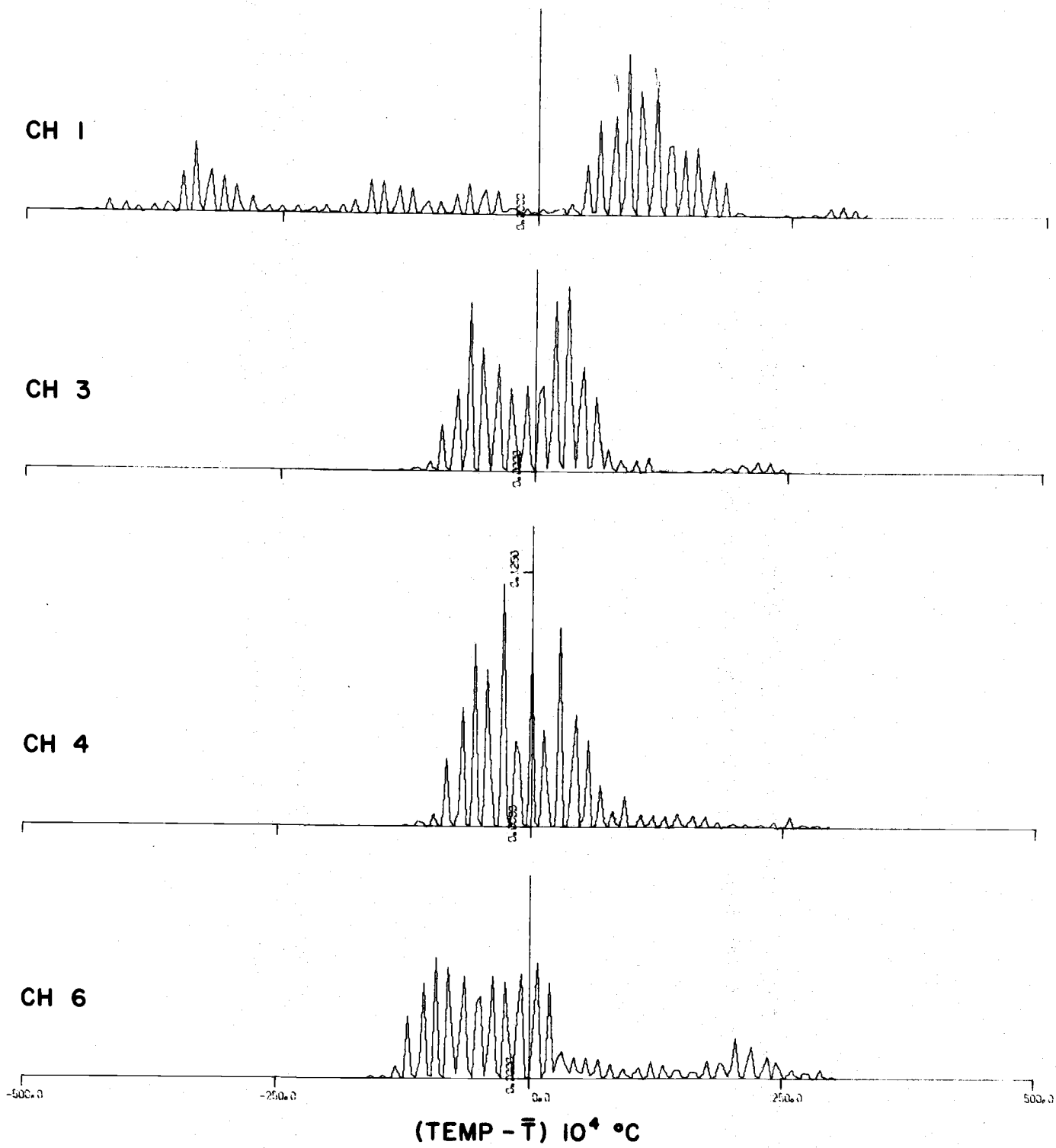


FIGURE 8
 PHASE I PROBABILITY DENSITY FUNCTIONS FOR CHANNELS 1,3,4, and 6

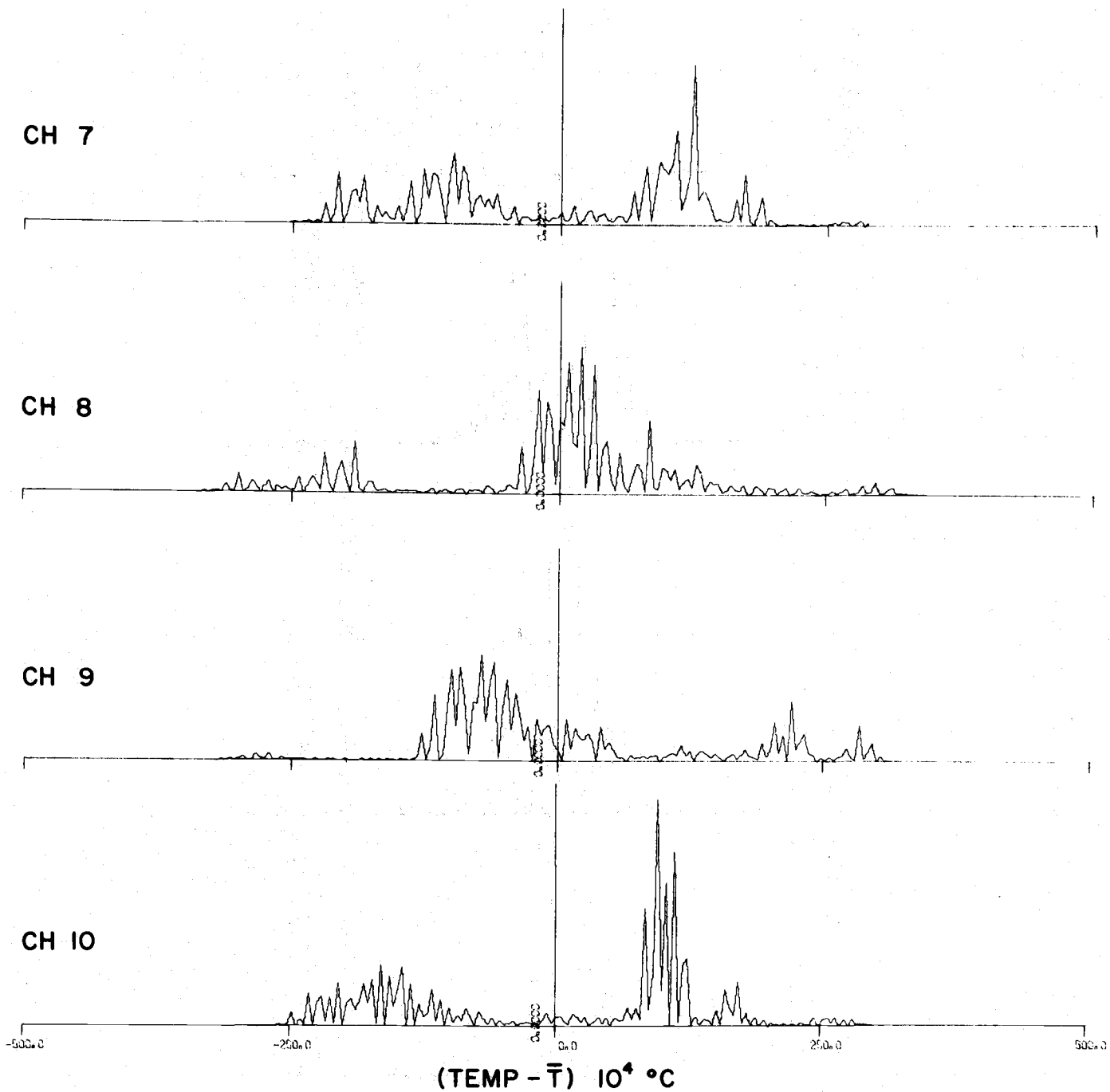


FIGURE 9
PHASE I PROBABILITY DENSITY FUNCTIONS FOR CHANNELS 7,8,9 and 10

CHANNEL 10

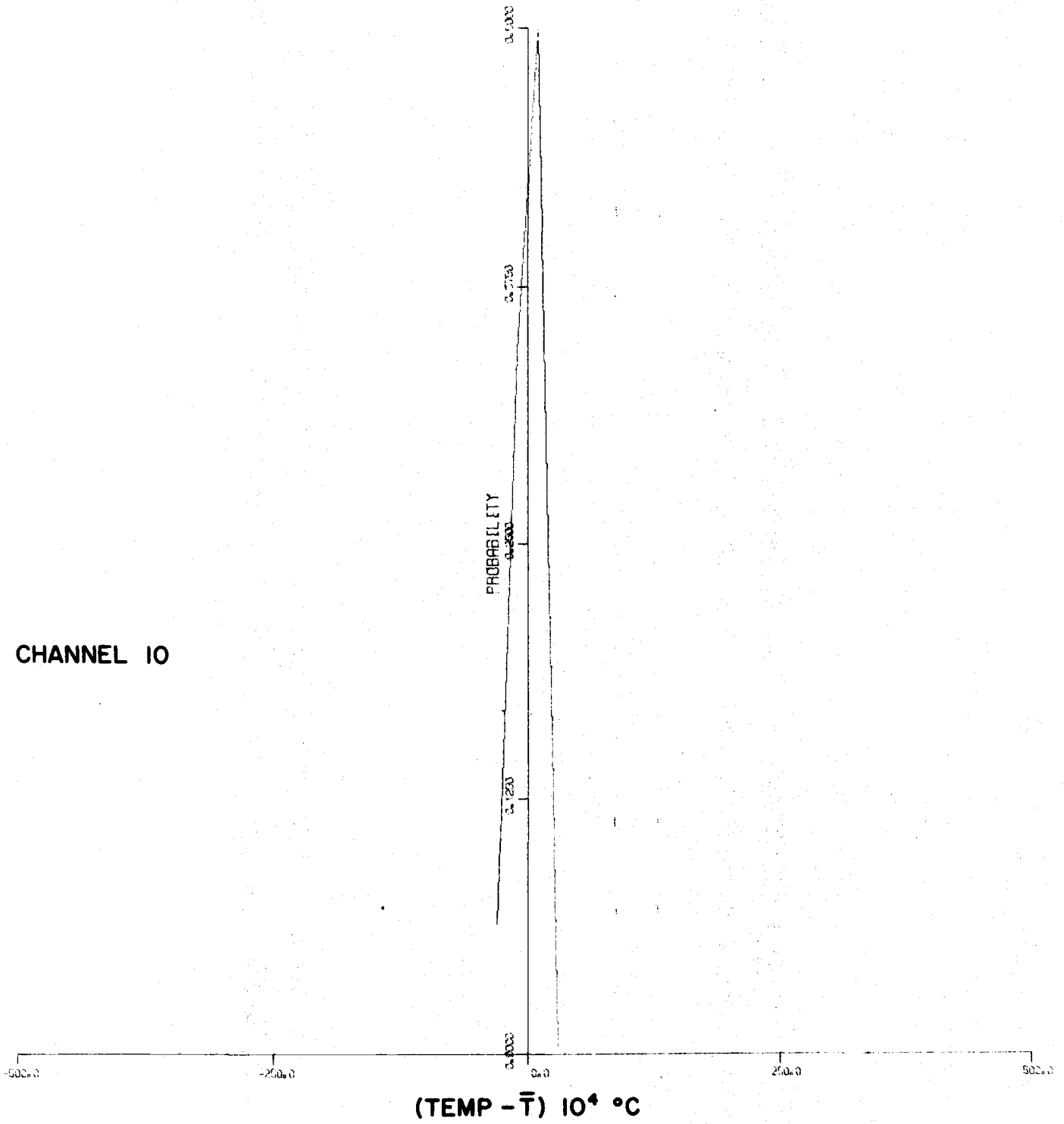


FIGURE 10
PHASE III(b) FILE 3 PROBABILITY DENSITY FUNCTION FOR CHANNEL10

and centered about this line. The latter would reflect the random effects induced by the electronic digitizing and recording equipment. A realistic approximation of the probability density of a thermistor subjected to a nearly uniform environmental temperature is available because we chose 3 files of 1000 consecutive values each for all channels in arriving at the field calibration constants. These files represent recordings of temperature which include both environmental and electronic fluctuations about the nominal environmental temperature. The third file observations from a depth of 287.5m, possessed the least variability - a standard deviation of approximately 0.001°C . For illustration purposes the probability density functions were computed from file 3 of the Phase III(b) recordings. As an example, refer to the probability density function for channel 10 shown in Figures 9 and 10. Figure 9 reveals a considerable number of observations were acquired when the thermistor was subjected to an environmental temperature of $100.0 \times 10^{-4}^{\circ}\text{C}$ above the mean, i.e. -0.0422°C . The latter value is arrived at through use of the accepted mean temperature for channel 10, Phase I (see Table III). Figure 10 reveals the probability density function when the same thermistor was subjected to a nearly uniform environmental temperature. From Figure 7 we observe that channel 10 experienced a temperature 0.0100°C in excess of the mean after the 654th observation (recall these are every tenth value, 654 here is equivalent to actual Phase I observation number 6540). Beginning at approximately observation 666 we note the presence of a reasonably well-mixed layer of temperature 0.0175°C below the mean. This layer moves away from the thermistor after a short time and the warmer layer appears again at approximately observation number 741. The thermistor remains in this

layer until observation number 816. This layer of -0.0422°C temperature surrounded the thermistor for approximately 1875 seconds ($75 \times 10 \times 2.5$ seconds) or approximately 31 minutes. This layer reappears several times, as revealed in Figure 7. Undoubtedly the passage of these well-mixed layers, with respect to the thermistors in the array, is a consequence of internal waves.

These data were also subjected to spectral analysis. Spectra were computed for each of the channels using a variety of lags (degrees of freedom). The observations were also prewhitened. For the purposes of this report we present the average normalized spectrum in Figure 11. The average is composed of channels 1,6,7,8,9 and 10 only. The observations from channels 3 and 4 did not contain sufficient steps to contribute to the spectrum statistics. The spectra were computed using 77 lags and have a band width resolution of 1.87 cph. By averaging the normalized spectra obtained from each of the sensors noted above, we are able to suppress variations caused by the statistical nature of the spectrum measurement. This technique has been used by various investigators, e.g. Cox (1966). The spectrum has a slope of approximately f^{-3} for frequencies less than 40 cycles/hr (periods greater than 90 seconds). The spectrum whitens at higher frequencies indicating the effects of noise within the system (environment plus electronics). The spectra of Phase III(b) observations are white over all frequencies. This finding substantiates our conclusion, derived from other considerations, that the three files of observations selected from the Phase III(b) recordings were suitable for computation of field calibration constants

B. Phase II (5-6 March, 1970)

The Phase II experiment was a repetition of Phase I but the array was about two meters deeper. The nine thermistors were located within the depth

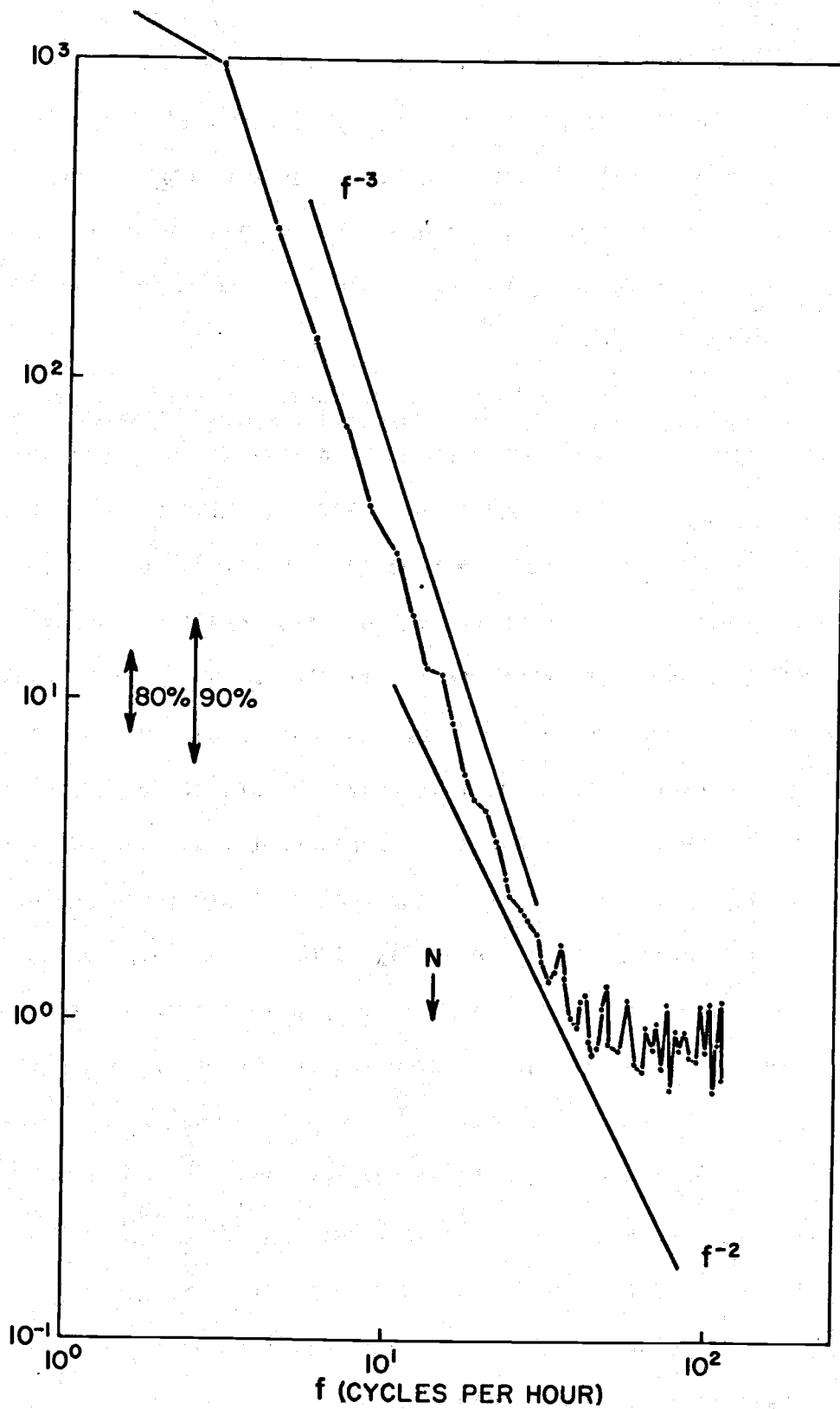


FIGURE 11
 PHASE I
 AVERAGE NORMALIZED SPECTRUM FOR
 CHANNELS 1,6,7,8,9 and 10

range 278m to 284m. There were 17,233 samples acquired from each of the 8 functioning thermistors, at a nominal sampling rate of once each 2.5 seconds.

The statistics summarizing these observations are presented in Table VI. The increase in temperature with increasing depth is apparent in column 3. The vertical gradient, based on the difference between the accepted mean temperatures of the shallowest and deepest thermistors, is 0.00932°C . This mean vertical gradient is in excellent agreement with that derived from the Phase I observations. (The thermistors were placed at depth intervals of exactly 76.2 cm and the total depth range sampled by the array was 6.095m. This exact value has been used for computations vice the approximate value of 6m).

The statistics contained in Table VI are presented graphically in Figure 12.

The time series of temperature observations produced by plotting every tenth value is presented in Figure 13. The format is described above under Phase I (for Figure 7). The magnitude of the temperature steps (difference in temperature of successive layers, or well-mixed zones) determined from Figure 13 are as follows: Channel 1, 0.024°C ; channel 3, 0.026°C ; channel 4, 0.026°C ; channel 6, 0.026°C ; channel 7, 0.026°C ; channel 8, 0.027°C ; channel 9, 0.029°C ; and, channel 10, no clearly defined steps. The approximate average value is 0.026°C , as was the case in Phase I. Unlike the Phase I observations, there were no instances when temperature differences of 0.013°C were persistent; however, there are a few individual cases where half step differences may have existed for short periods. There were no

TABLE VI

Summary of Temperature Statistics ($^{\circ}\text{C}$) - Phase II

Channel Number	Uncorrected Mean	Field Cal. Const.	Accepted Mean	Standard Deviation	Min. Temp.	Max. Temp.	Temp. Range
1	-.7511	.6507	-.1004	.0042	-.1259	-.0835	.0835
3	-.8325	.7348	-.0977	.0096	-.1119	-.0681	.0438
4	-.9591	.8715	-.0876	.0134	-.1089	-.0644	.0445
6	-.9229	.8490	-.0739	.0088	-.1076	-.0407	.0669
7	-.5879	.5204	-.0675	.0107	-.0984	-.0383	.0601
8	-.6575	.5991	-.0584	.0140	-.0833	-.0360	.0473
9	-.5918	.5466	-.0452	.0089	-.0795	-.0297	.0498
10	-.5698	.5262	-.0436	.0032	-.0507	-.0313	.0194
						Average	.0519

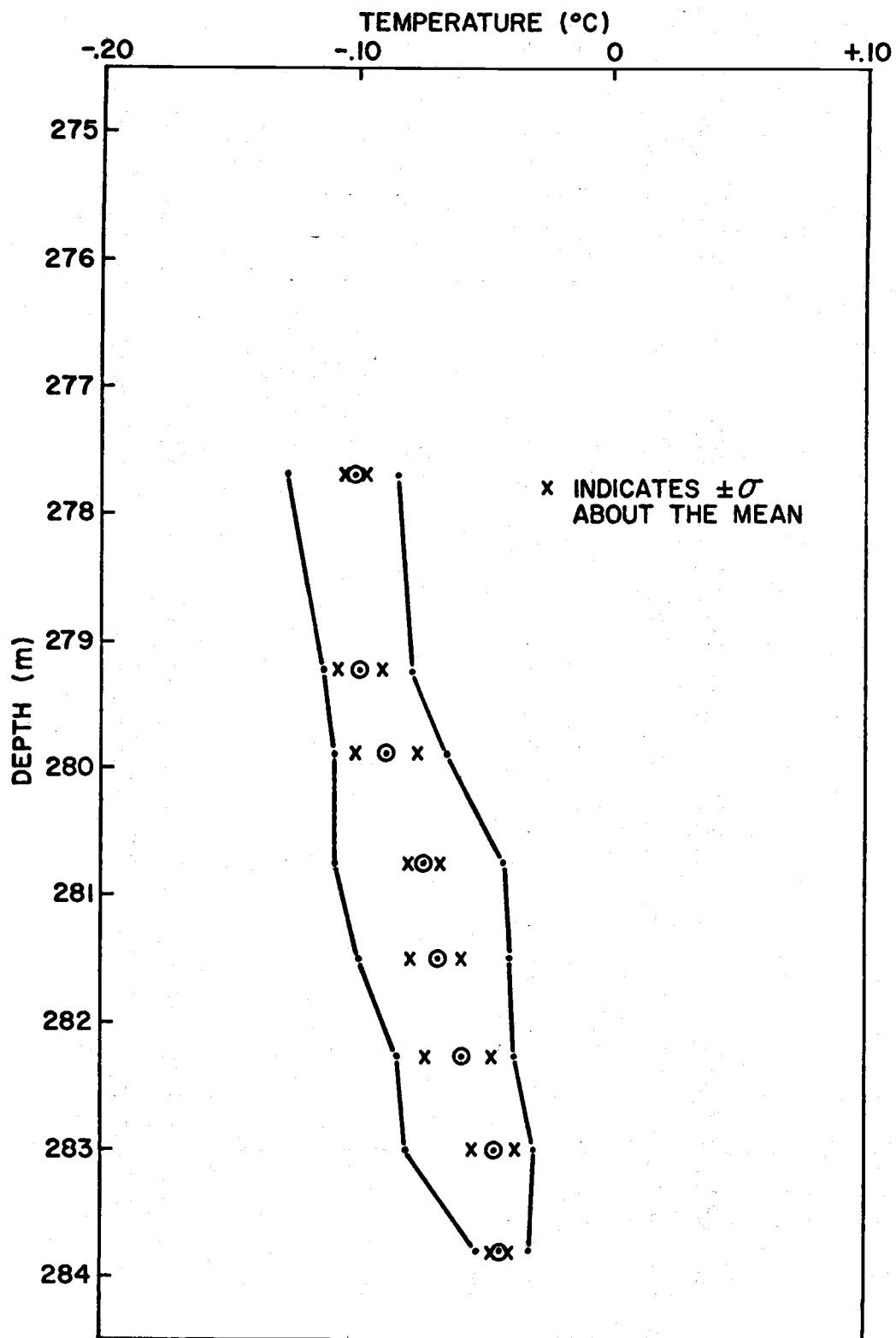


FIGURE 12
 PHASE II
 TEMPERATURE STATISTICS

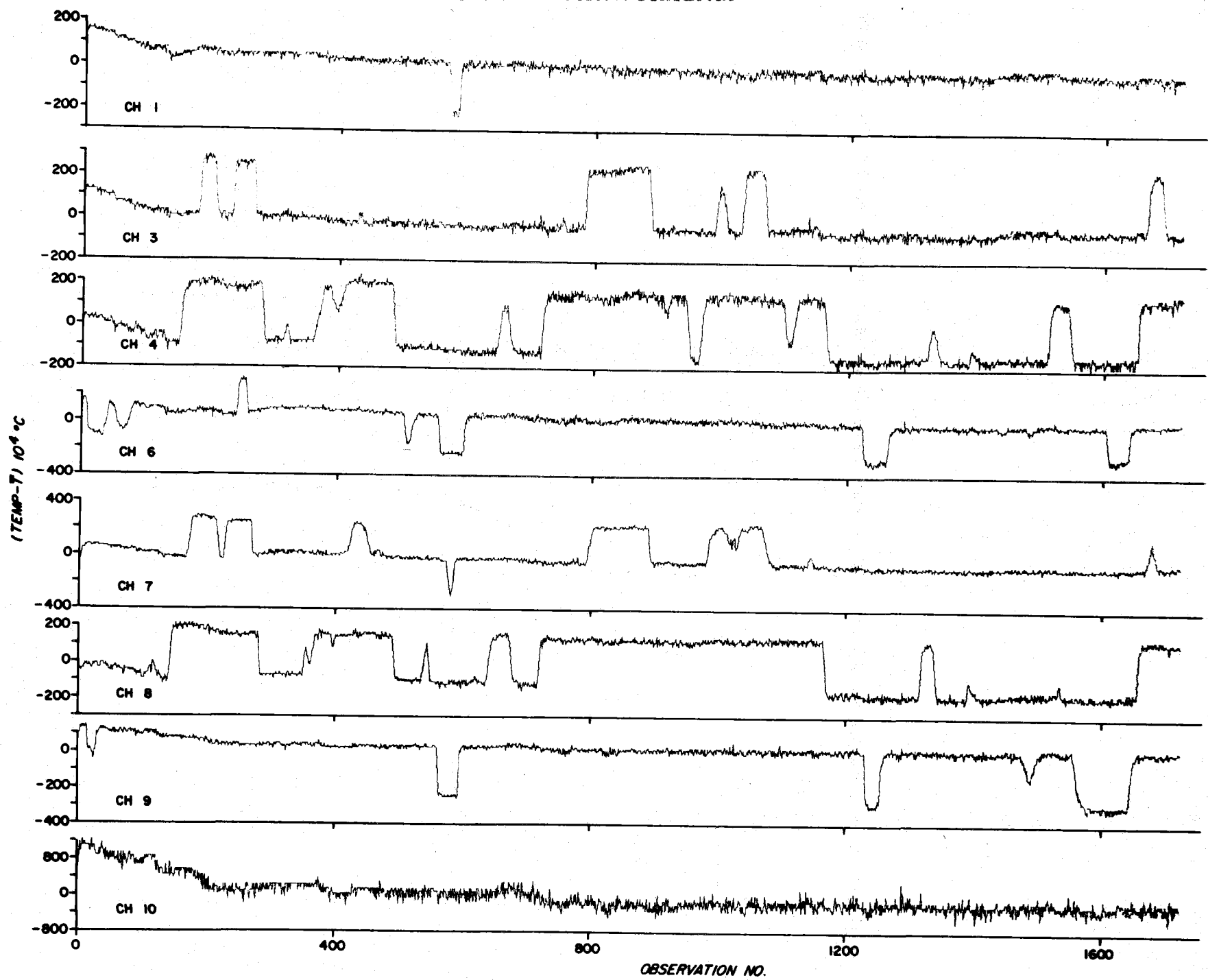


FIGURE 13
 PHASE II (TEMPERATURE \bar{T}) 10^4 °C FOR EVERY 10th SAMPLE VALUE

temperature steps in the channel 10 data and only one in the channel 1 data. Channels 3 and 4 of the Phase I data were similar (see Figure 7).

Using the average step value of 0.026°C , in conjunction with the temperature range resulting from the difference between the minimum temperature from channel 1 and the maximum temperature from channel 10, we conclude that there are approximately 3.6 vertical temperature steps within the depth interval sampled by the array. Using the same procedure we concluded there had been approximately 5.3 vertical temperature steps observed in the Phase I data. If the temperature difference (step) of 0.026°C is a correct approximation, and if the mixed layers were of similar thickness during Phases I and II then one might tentatively speculate that the internal wave heights encountered during Phase I (4 March, 1970) were greater than those encountered during Phase II (5-6 March, 1970).

Temperature spectra were computed for channels 3,4,6,7,8 and 9 of the Phase II data using the resampled observations (every tenth value of the original record). Spectra were not computed for the channel 1 or channel 10 observations due to absence of a stepped temperature structure. An average of these individual spectra was computed. This average spectrum is presented in Figure 14. Comparison of Figures 11 and 14 reveals marked similarity between the Phase I and Phase II time series. A slope of f^{-3} appears to represent the spectra for frequencies between 2.9 and 40.0 cph (20.6 to 1.50 minute periods). A spectral slope of f^{-3} was observed by Haurwitz et al. (1959) for temperature data acquired off Castle Harbour, Bermuda.

A spectral slope of f^{-2} has been theorized by Phillips (1971) and Reid (1971) for the case of a stepped thermal structure disturbed by a random field of internal waves. The line corresponding to an f^{-2} spectral slope has been included in Figures 11 and 14. It seems apparent that the only

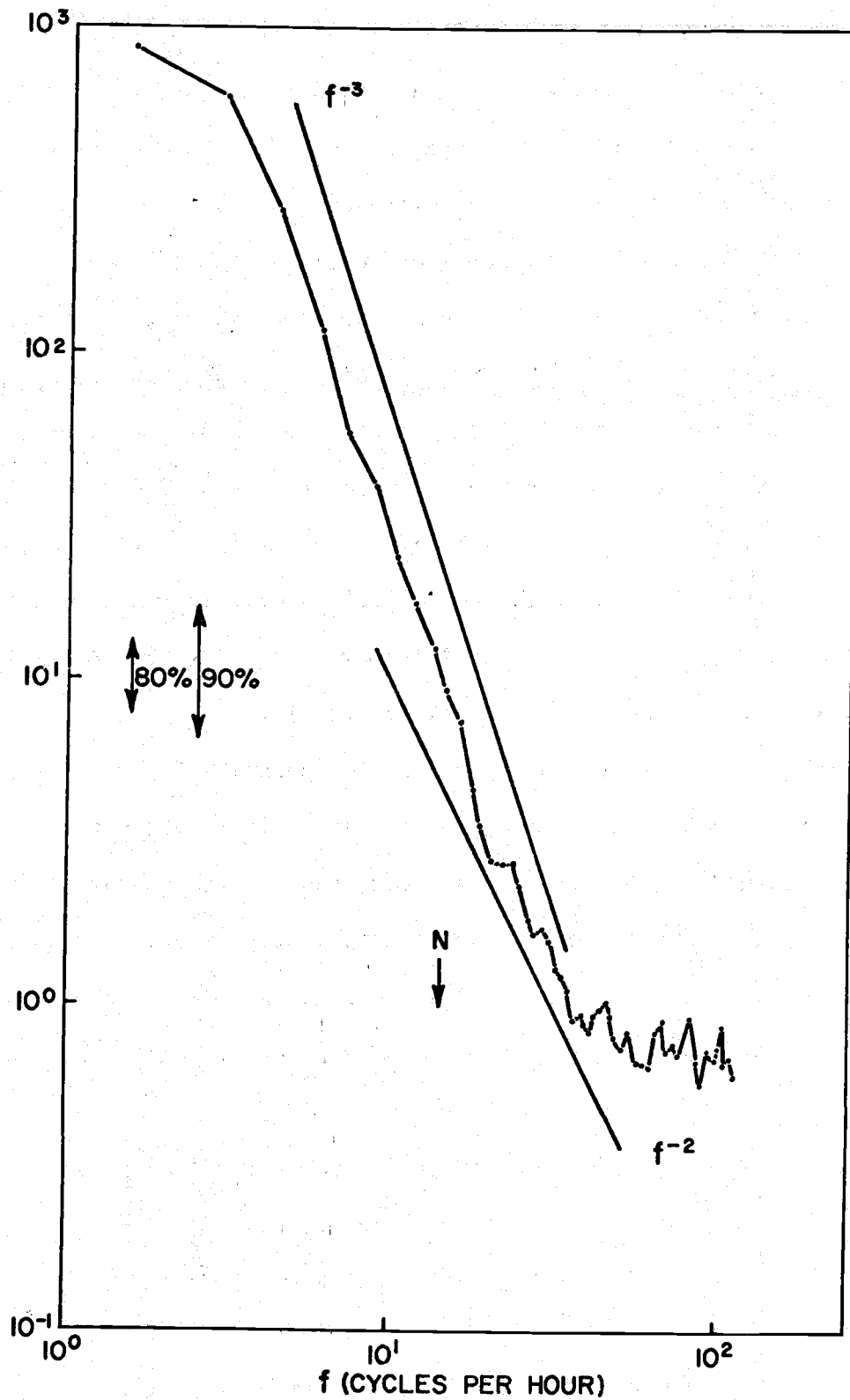


FIGURE 14
 PHASE II
 AVERAGE SPECTRUM FOR CHANNELS
 3,4,6,7,8 and 9

region of the spectra which may be characterized by an f^{-2} lies in the approximate range 18 to 40 cph (3.33 to 1.50 minute periods).

We believe that the presence of f^{-3} and f^{-2} slopes in the Phase I and Phase II spectra may be explained. If our interpretation given below is correct, these data reveal a very interesting aspect of ocean measurements which, to our knowledge, has not been previously reported.

It is known that spectra of internal waves display a high frequency termination at the local Brunt-Väisällä frequency, N . This frequency is given by the expression: $N = \left\{ -\frac{g}{\rho_0} \frac{\partial \rho}{\partial z} - \frac{g^2}{c^2} \right\}^{\frac{1}{2}}$, where g is the local acceleration of gravity, ρ_0 the mean density, $\frac{\partial \rho}{\partial z}$ the density gradient (z positive upward) and c , the speed of sound. The Brunt-Väisällä frequency is the natural frequency at which a fluid element will oscillate when given a small displacement from its equilibrium position.

This frequency has been computed using the data presented in Figure 5. Two computations of N were made. The first value, $N = 14.2$ cph, was given using the linear interpolation of temperature and salinity observations acquired on 14 March, 1970. The second value, $N = 14.0$ cph, was obtained using the actual observations of temperature and salinity versus depth. These values are very similar considering the dependence of N on the vertical gradient of density. The value of $N = 14$ cph has been indicated in Figures 11 and 14. This value is of course strongly dependent upon the values of density computed from temperature, salinity and depth. A frequency of 18 or 19 cph can be derived if one adjusts the observed temperature and salinity values within their measurement resolution.

Spectra obtained from a fixed thermistor in the presence of a disturbed layered (stepped) structure will extend, in the frequency domain, beyond N. Their high frequency termination will occur at the frequency, say M, where M is the inverse of the time required for passage of the temperature step (sheet) past the thermistor. In development of this concept Phillips (1971) points out that observational limitations, such as resolution of the probes, may terminate the spectra at frequencies less than M. As noted above, the highest frequency which is characterized by an f^{-2} slope is approximately 40 cph. If $M = 40$ cph, we compute the time for passage of a temperature step (sheet) to be approximately 90 seconds.

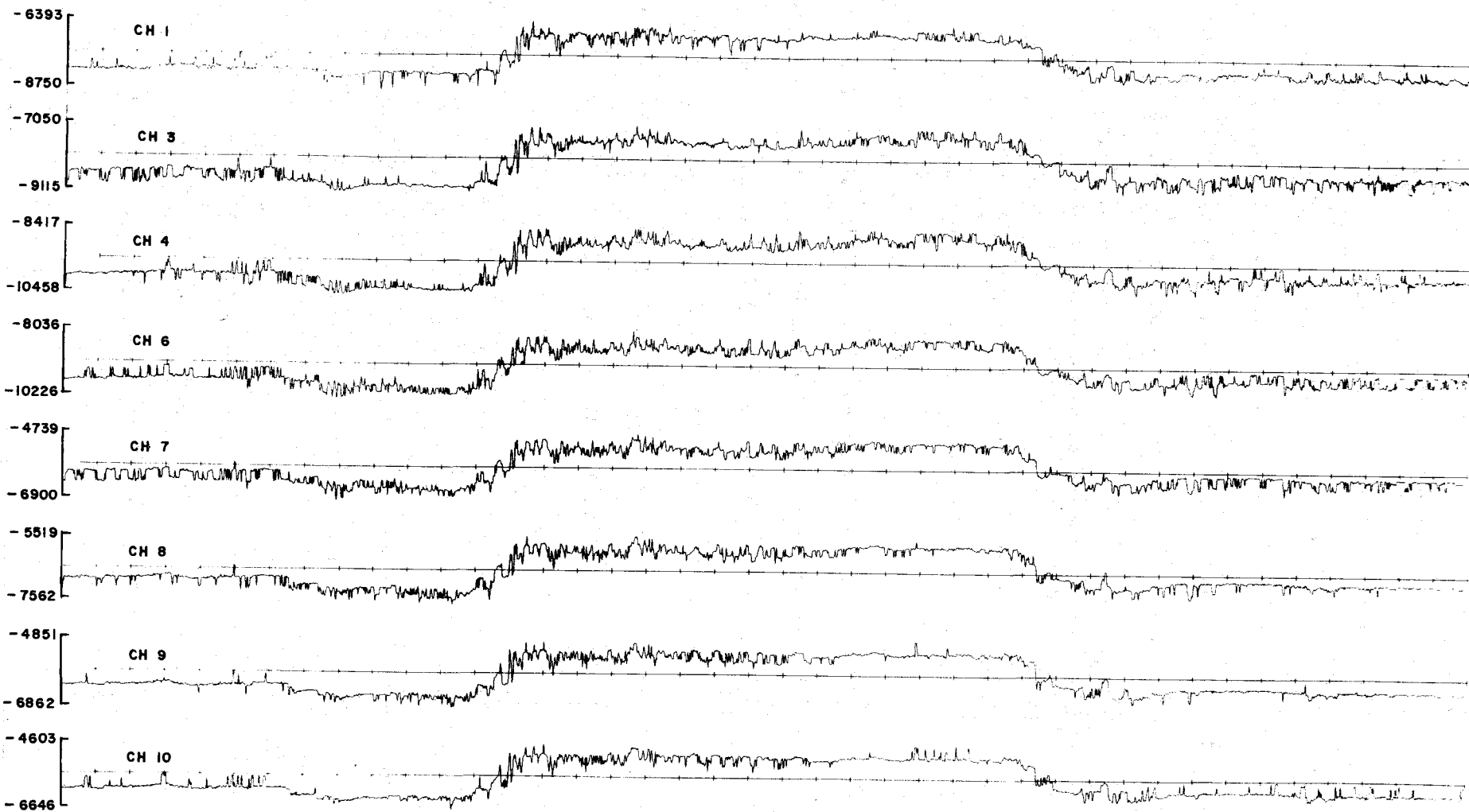
In summary, we suggest that the spectra computed from the Phase I and Phase II observations reveal the presence of internal waves over frequencies less than N, where the spectral density decreases in proportion to f^{-3} . At frequencies greater than N, where the spectral density decreases in proportion to f^{-2} , we encounter the effects of vertical oscillation of the stepped thermal structure past the thermistors. This portion of the spectra therefore describes the latter and not the internal waves themselves. Stated another way, the spectral behavior at frequencies greater than N is a consequence of the presence of the stepped structure.

Caution must be used in interpretation of the results listed above. The theoretical spectral density decay in proportion to f^{-2} is applicable to observations acquired from a fixed probe or to one moving horizontally at a fixed velocity. In our case the probe is reasonably well fixed in the vertical but is dragged about as the ice island moves. Additionally, one would expect some horizontal flow of the fluid relative to the horizontal motion of the ice island. Based on the reasonable results depicted in Figure 11 and 14 these various contamination effects must have collectively been small.

C. Phase III(a) (8 March - 5 April, 1970)

During Phase III(a) the thermistors on the array were suspended beneath the ice between depths of 278m and 284m. The vertical spacing of 76.2cm was retained as in Phases I and II. As during the previous Phases, the channel 2 thermistor failed to function properly. As noted earlier, the array was raised and lowered several times during the duration of Phase III (a). The times of these events are shown in Figure 3. The DART was internally configured during this Phase to sample the thermistors once every 10 minutes. Control was provided by an Acutron clock with a 10 minute contact switch. This clock did not function properly during the experiment. Through analysis of the precise times of the raising/lowering events and the perturbations thereby introduced in the temperature time series, the correct nominal sampling rate has been derived as 19.7 minutes. According to our analysis, the clocked sampling interval increased steadily from the intended amount of 10 minutes to the actual amount of 19.7 minutes, achieving the latter within approximately 6 hours. As noted in section II, the Acutron clock had been cold-chamber tested prior to use. These tests revealed only miniscule deviations over a period of 30 days. If the raising/lowering events had not been incorporated and suitably spaced in the experiment we could not have analyzed the data in the time and frequency domains. The total duration of the experiment was limited by failures within the DART on 5 April, 1970.

The Phase III(a) temperature series suited for analysis consist of 2048 values from each of the functioning channels. These observations are plotted in Figure 15. The temperature recordings on the ordinates are



-40-

FIGURE 15
PHASE II TEMPERATURE SERIES (TEMPERATURE VALUES NOT CONVERTED)

uncorrected and should be disregarded. The tick marks along the abscissae indicate intervals of 50 data points (approximately 16.4 hours).

Aside from the obvious presence of temperature fluctuations, attributable to the existence of a stepped or layered thermal structure, Figure 15 reveals a "plateau" of warmer water within the center region of the data. We feel that this plateau was introduced by movement of the ice island and therefore depicts a horizontal gradient in the thermal structure. The location of the ice island at the times of proposed entering (up ramp) and exiting (down ramp) of this warmer region are shown in Figure 4. It should be noted that these ramps are not associated with times of the raising/lowering events.

Our first step in preparing these data for analysis was removal of this warm plateau. This was deemed necessary in support of our purpose of studying fluctuations in temperature rather than spatial gradients of temperature.

Removal of the plateau observed in each channel was accomplished in the following fashion. In this example we treat the observations of an individual channel. The original observations were divided into the following five segments: (1) observations 1 through 621; (2) observations 622 through 680 (up ramp); (3) observations 681 through 1381; (4) observations 1382 through 1484 (down ramp); and, (5) observations 1485 through 2048. Average values were computed for segments 1,3 and 5. Linear interpolations between the averages of segments 1 and 3 and 3 and 5 were computed for segments 2 and 4, respectively. The respective averages and interpolations between averages were subtracted from the original observations. The weighted mean value was computed using the averages of segments 1,3 and 5. This base (DC) level for the channel was compared with the overall average

value of the observations after plateau removal. The base DC level and overall average after plateau removal differ by no more than $4 \times 10^{-4}^{\circ}\text{C}$. The values resulting from these computations are presented in Table VII. The vertical temperature gradient, based upon the accepted mean temperatures of the shallowest and deepest thermistors, is $0.01181^{\circ}\text{Cm}^{-1}$. The similarly derived mean vertical gradients, for the Phase I and Phase II observations, were $0.00986^{\circ}\text{Cm}^{-1}$ and $0.00932^{\circ}\text{Cm}^{-1}$, respectively.

The accepted average temperatures for each of the segments and channels are presented in Table VIII. The differences in average segment temperatures indicate the magnitude of the up and down ramps of the temperature plateau. By incorporating the distance traversed by the ice island (Figure 4) during observation of these ramps, we conclude that spatial gradients of the order 0.1°C/nm were observed. This value may seem, intuitatively at least, to be rather high. The absence of comparable data should be considered however, before the argument of spatial change can be rejected. One notes, again from Table VIII that the implied spatial gradient of temperature (columns 5 and 6) is not uniform over the depth interval sampled by the array. The average up-ramp and down-ramp gradients are 0.1174°C and 0.1022°C , respectively. These values indicate that the horizontal gradients of the isotherms sampled by the array are not uniform. This may be expected in an instance of relatively weak baroclinic flow.

Various numerical filters were applied to the original observations in order to remove the plateau. These filtering techniques removed the plateau but resulted in some distortions of the frequency content of the original records. Therefore, all filtering procedures were terminated.

Statistics from the Phase III(a) data with the plateau removed are presented

TABLE VII

Phase III(a) - Plateau Removal ($^{\circ}\text{C}$)

Channel Number	Ave. Segment 1	Ave. Segment 3	Ave. Segment 5	Base DC Level	Mean With Plateau Removed	Diff. Between Col. 5&6	Accepted Field Cal. Const.	Accepted Mean Temp
1	-.8152	-.6868	-.8083	-.7655	-.7651	4	.6507	-.1144
3	-.8760	-.7505	-.8600	-.8247	-.8244	3	.7348	-.0896
4	-.10039	-.8803	-.9863	-.9528	-.9525	3	.8715	-.0810
6	-.9729	-.8520	-.9519	-.9218	-.9214	4	.8490	-.0724
7	-.6287	-.5162	-.6106	-.5815	-.5813	2	.5204	-.0609
8	-.7002	-.5902	-.6844	-.6547	-.6546	1	.5991	-.0555
9	-.6385	-.5294	-.6261	-.5943	-.5941	2	.5466	-.0475
10	-.6136	-.5042	-.6005	-.5691	-.5688	3	.5262	-.0426

TABLE VIII

Magnitude of Temperature Plateau ($^{\circ}\text{C}$)

Channel Number	Accepted Ave. Segment 1	Accepted Ave. Segment 2	Accepted Ave. Segment 3	$T_3 - T_1$	$T_3 - T_5$
1	-.1645	-.0361	-.1576	.1284	.1215
3	-.1412	-.0157	-.1252	.1255	.1095
4	-.1324	-.0088	-.1148	.1236	.1060
6	-.1239	-.0030	-.1029	.1209	.0990
7	-.1083	+.0042	-.0902	.1125	.0944
8	-.1011	+.0089	-.0853	.1100	.0942
9	-.0919	+.0172	-.0795	.1091	.0967
10	-.0874	+.0220	-.0743	.1094	.0963
			Average	.1174	.1022

Average Spatial Gradient

 $T_3 - T_1$ (up-ramp), .0835 $^{\circ}\text{C}/\text{nm}$ $T_3 - T_5$ (down-ramp), .1022 $^{\circ}\text{C}/\text{nm}$

TABLE IX

Summary of Temperature Statistics ($^{\circ}\text{C}$) - Phase III(a)

Channel Number	Accepted Mean	Standard Deviation	Min. Temp.	Max. Temp.	Temp. Range
1	-.1144	.0144	-.1891	-.0473	.1418
3	-.0896	.0179	-.1439	-.0322	.1117
4	-.0810	.0191	-.1363	-.0137	.1226
6	-.0724	.0203	-.1324	-.0120	.1204
7	-.0609	.0195	-.1309	-.0077	.1232
8	-.0555	.0174	-.1190	-.0055	.1135
9	-.0475	.0150	-.1110	+.0138	.1248
10	-.0426	.0151	-.1048	+.0149	.1197
				Average	.1222

In Table IX and illustrated in Figure 16. These basic statistics display greater variability than those obtained from the Phase I and Phase II observations. This result is to be expected due to the greater duration of the Phase III(a) experiment. Aside from the effects of spatial changes introduced by ice island motion, one would expect the occurrence of greater vertical oscillations. The effects of the latter can be appreciated by noting: (1) the temperature ranges of the Phase III(a) observations average approximately 0.05°C greater than those of the Phase I and Phase II; and, (2) a single temperature step (sheet) represents an approximate temperature difference of 0.026°C . Therefore, addition of but two more temperature steps would increase the observed temperature range to the levels shown in Table IX. One of the more interesting aspects of these data is the rather small number of temperature steps which have been observed. Using a temperature difference of 0.026°C to represent a single step, the thermistors encountered slightly more than two steps during each of Phases I and II and less than 5 steps during Phase III(a).

The probability density functions were computed for each channel. The values of probability density observed in Phase III(a) were lower than those for Phases I and II, because a greater range of temperatures was encountered. As the duration of the experiment was extended, and more temperature steps passed the thermistors, the proportional amount of time at any single temperature diminished. Further increases in duration of the experiment, under identical environmental circumstances, will not lead to a uniform probability density function (equal probability density for each temperature encountered) because the step regions (sheets) are thinner than the well-mixed layers surrounding them. Consequently, and in spite of

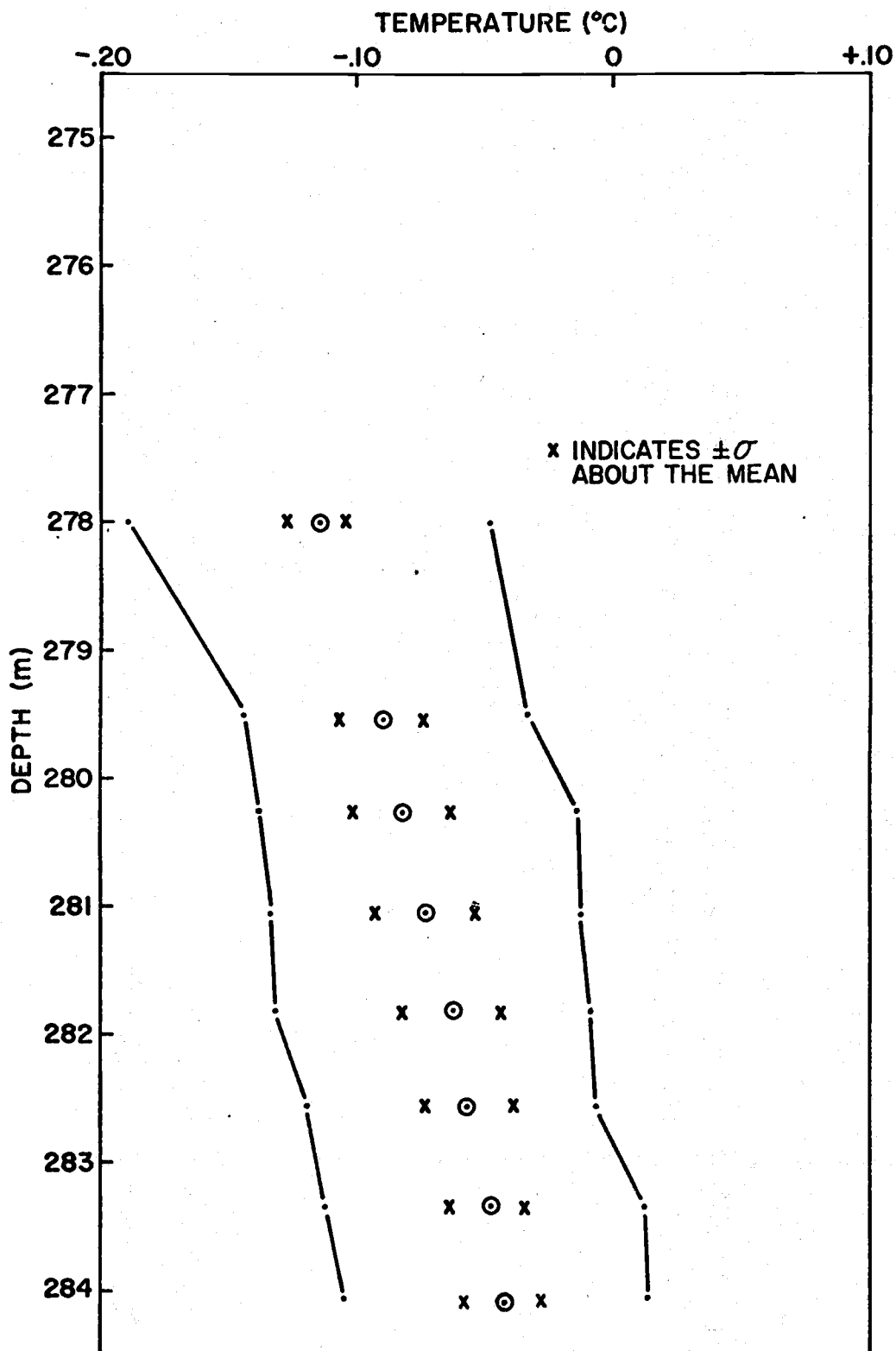


FIGURE 16
PHASE III(a)
TEMPERATURE STATISTICS

continual oscillation of the stepped thermal structure past the thermistors, the thermistors will be exposed to the temperatures of the layers more than to those of the sheets.

Spectra have been computed using the Phase III(a) time series. Of these we have chosen to present (Figure 17) the average (among channels) normalized spectrum (82 lags). It is noted that only every other spectral estimate has been plotted for frequencies higher than 0.7 cph. This has been done solely for convenience. The band width resolution of the spectrum is 0.0373 cph. The average spectrum reveals a general decrease in spectral density in proportion to f^{-1} . Portions of the spectrum may appear to possess an f^{-2} slope. These regions are relatively confined in frequency band width and are probably not truly characteristic of the spectrum.

The inertial frequency ($f_I = 0.083$ cph) is noted on Figure 17. Two other relative peaks in the spectrum occur at approximately 0.24 and 0.40 cph. Cox (1966) observed similar phenomena in temperature time series obtained in deep water off San Diego. He attributes them to overtones of the semidurnal oscillations. In our case these semidurnal oscillations include f_I . In interpreting the spectrum the reader is cautioned to recall that the ice island has undergone considerable motion during this phase of the experiment. A spectral analysis of ice island motion would seem to be in order, prior to attempting further analysis of the Phase III(a) spectrum. There was considerable N-S, E-W motion at what would be relatively small wave numbers. Analysis of larger wave numbers, which would describe motion at the inertial period, would require use of ice island positioning data taken more frequently than ours.

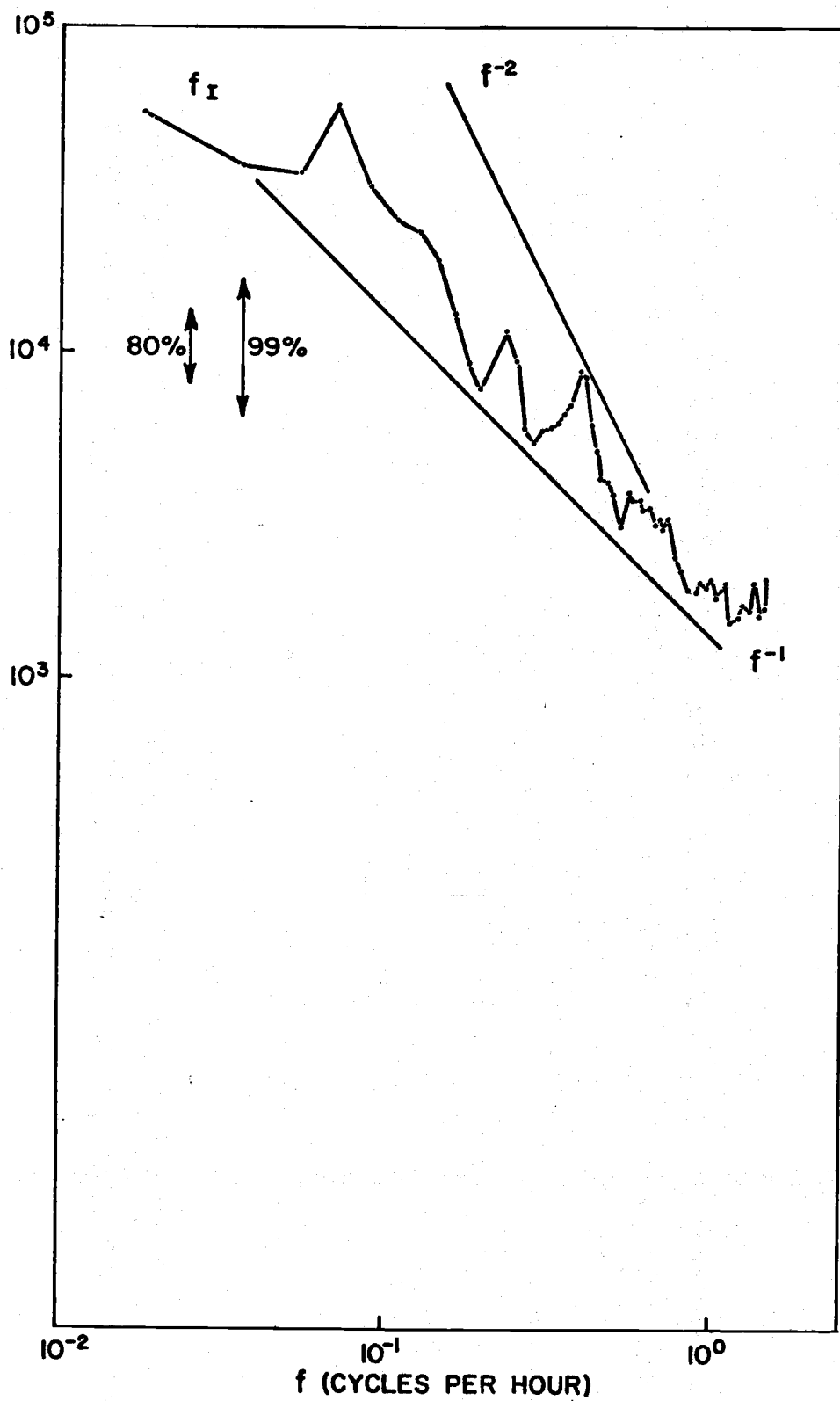


FIGURE 17
 AVERAGE NORMALIZED SPECTRUM FOR
 PHASE III(a)

The fact that the nominal sampling time for the Phase III(a) series was nearly twice as long (19.7 versus 10 minutes) as intended, minimizes the overlap hoped for between the Phases I and II and Phase III(a) observations.

In summary the spectra from these three Phases reveal a spectral decay with respect to frequency of: (a) f^{-1} , for frequencies less than 1.3 cph; (b) f^{-3} , for frequencies between 1.3 cph and the Brunt-Väisälä frequency (N); and, (c) f^{-2} , for frequencies greater than N.

It is noted that the f^{-1} decay is in general agreement with the findings of Cox (1966) for depth averaged normalized spectra computed from temperature time series obtained off San Diego. The f^{-3} decay is in general agreement with the observations of Yearsley (1966) obtained from a depth of 60m in the Arctic.

D. Phase IV (17 April, 1970)

The Phase IV observations have not been analyzed. These observations were acquired from the thermistor array while suspended at depths between 600 and 606m. Observations were recorded every 2.5 seconds, as in Phases I and II. For each of the 8 functioning channels there are approximately 14,000 values available for analysis.

The original magnetic tape recording has been read and a listing of values produced. The listing indicates sporadic malfunctioning of the DART. These malfunctions affect a total of some 1000 values. Some effort will be required to determine the best method for removing these bad values. Our success at resampling the original observations (Phase I and II) at every tenth value enables us to delete bad values which occur in sequences of less than 9 values. There are some sequences which incorporate nearly 100 values. In these instances the values could either be deleted altogether,

resulting in a spliced time series, or new values could be interpolated, on the basis of acceptable surrounding values. Furthermore, it is possible to analyze original data in segments of a few thousand values each. The results could then be combined using a suitable averaging technique.

Correction of the original values, using the field calibration constants (Table II) indicates in situ temperatures in the range 0.32°C to 0.28°C . This range is in excellent agreement with the temperatures acquired from the ocean station observations obtained during the same period. The temperatures diminish with increasing depth over the 6m interval which is also in keeping with the ocean station observations. The approximate ranges of temperature, observed over the span of some 15,000 samples (10.4 hours), are 0.01°C to 0.03°C with one exception. The channel 1 observations span the range: 0.46°C to 0.53°C . These values are typical for depths of 500m to 550m. Though one might argue the influence of very large internal waves it is doubtful that such could exist and, at the same time, influence only the thermistor at 600m depth. Therefore, these observations must be considered questionable.

V. RECOMMENDATIONS

The spectral properties of the Phase I and Phase II observations should be studied in more detail. In particular, the question of coherence among the channels should be addressed. These data should also be analyzed to determine the portion of time during which the thermistors were within layers versus sheets. The data should be analyzed in light of theoretical treatments of internal wave propagation within a stepped thermal structure.

The Phase III(b) observations are best suited for analysis of low-frequency internal oscillations of the vertical thermal structure. Their

value for such study, however, could only be realized if the ice island motions were suitably treated. The question of sampling rate stability remains. The nominal sampling interval of 19.7 minutes is known to possess a variation of up to 5%. This smearing effect may be small, compared to the alterations induced by horizontal motion of the ice island, but nevertheless, it is present and does diminish the validity of the observations.

The Phase III(a) observations may lend themselves to analysis for among channel coherence. Initial work has been undertaken. Specifically, we have developed numerical filters for use with the data which will enable one to compare, among channels, temperature fluctuations within various frequency bands.

The Phase IV observations should be studied to determine the nature of temperature fluctuations within the deeper layers. The analysis techniques proposed above for the Phase I and II data also apply to the Phase IV data.

Repetition of the experiment, as originally designed, would be of value in assessing the influences of shear in producing and maintaining the stepped thermal structure. It would seem prudent and justifiable, in view of the data presented here, to conduct such an experiment over a shorter time span than one month. Our findings indicate that a time span of approximately one day may be quite sufficient. This would require rapid sampling and concomitant high resolution current measurements.

ACKNOWLEDGMENTS

The authors are grateful to a number of individuals from various organizations for invaluable assistance in this work. The equipment utilized for the experiment was provided by Project Themis, Oregon State University. Support while aboard ice island T-3 and shipping costs were provided by the Arctic Institute of North America, under contractual arrangements with the Office of Naval Research (Project number ONR - 432). A portion of the necessary computer time as well as computer programs written by Dr. Thomas Davis have been provided by the Naval Oceanographic Office. Ocean station observations were provided by Dr. T.S. English, University of Washington. Positioning data for ice island T-3 were provided by Dr. K. Hunkins, Lamont-Doherty Geophysical Observatory.

Special appreciation is extended to Mr. John Dawson, USC biologist aboard ice island T-3, for his able assistance in deploying and recovering the array during each Phase of the experiment. Dr. Don Durham, Texas A & M University, was successful in translating the original digital tape recordings - a task which we were totally unable to perform with the equipment available at Oregon State University. Mr. J. Sater of the Arctic Institute of North America is gratefully acknowledged for his infinite patience and understanding displayed over the long period required for preparation of this report.

REFERENCES

- Cooper, H.H.N.
 1967. Stratification in the deep ocean. *Sci. Prog., Orf.*, 55: 73-90
- Cox, Charles S.
 1966. Energy in Semidurnal Internal Waves. *Proceedings of the Symposium on Mathematical-Hydrodynamical Investigations of Physical Processes in the Sea, Moscow.*
- Haurwitz, B., H. Stommel and W.H. Munk.
 1959. On Thermal Unrest in the Ocean. *Rosby Memorial Volume, New York, Rockefeller Institute Press: 74-94.*
- Lovett, J.R.
 1968. Vertical temperature gradient variations related to current shear and turbulence. *Limnol. Oceanogr.* 13(1): 127-142.
- Neal, Victor T., Stephen Neshyba and Warren Denner
 1969. Thermal stratification in the Arctic Ocean. *Science*, 166: 373-374.
- Neal, V.T., Stephen Neshyba and Warren Denner
 1971. Temperature microstructure in Crater Lake, Oregon. *Limnol. Oceanogr.* 16: 695-700.
- Neal, Victor T., Stephen Neshyba
 1972. Some temperature microstructure anomalies in the Arctic. *JGR* 78(15): 2695-2701.
- Neshyba, Stephen, V.T. Neal and Warren Denner
 1969. The significance of temperature stratification in the Arctic. *Proc. of Symposium on Military Oceanography* 457-471.
- Neshyba, Stephen, V.T. Neal and Warren Denner
 1971. Temperature and conductivity measurements under Ice Island T-3. *JGR* 76(33): 8107-8120.
- Neshyba, Stephen, V.T. Neal and Warren Denner
 1972. Spectra of internal waves; in situ measurements in a multiple-layered structure. *J. Phys. Oceanogr.* 2(1): 91-95.
- Phillips, O.M.
 1971. On Spectra Measured in an Undulating Layered Medium. *Journal of Physical Oceanography*, 1(1): 1-6.
- Reid, R.O.
 1971. A Special Case of Phillips' General Theory of Sampling Statistics for a Layered Medium. *Journal of Physical Oceanography*, 1(1): 61-62.

- Stommel, Henry and K.N. Fedorov
1967. Small scale structure in temperature and salinity near Timor and Mindanao. *Tellus*, 19(2): 306-325.
- Tait, R.T. and M.R. Howe
1968. Some observations of thermohaline stratification in the deep ocean. *Deep-Sea Res.*, 15: 275-280.
- Turner, J.S. and Henry Stommel
1964. A new case of convection in the presence of combined vertical salinity and temperature gradients. *Proc. N.A.S.*, 2: 49-53.
- Turner, J.S.
1965. The coupled turbulent transports of salt and heat across a sharp density interface. *Int. J. Heat Mass Transfer*, 8: 759-767.
- Turner, J.S.
1967. Salt fingers across a density interface. *Deep-Sea Res.* 14: 599-611.
- Turner, J.S.
1968. The influence of molecular diffusivity on turbulent entrainment across a density interface. *J. Fluid Mech.*, 33: 639-656.
- Woods, J.D.
1968. Wave-induced shear instability in the summer thermocline. *J. Fluid Mech.*, 32: 791-800.
- Yearsley, J.R.
1966. Internal Waves in the Arctic Ocean. Technical Report No. 5 CU-5-66-Nonr 266(82), Lamont Geological Observatory, Palisades, New York.